The EicC project in China

Yutie Liang

Institute of Modern Physics, CAS, China

On behalf of the EicC Discussion Group

08/20/2019, Hadron 2019
Guilin, China

Outline

- **Introduction**

  polarized Electron ion collider in China (EicC)

- **Physics programs in EicC**

  PDFs, TMDs, GPDs, Proton Mass,

  pi/K structure function, Hadron Spectroscopy

- **Current status**

- **Summary**

Introduction

- QCD is successful (in general). More than 90% of visible matter in nature governed by strong interaction QCD.

- But not perfect yet. Some fundamental problems to be addressed

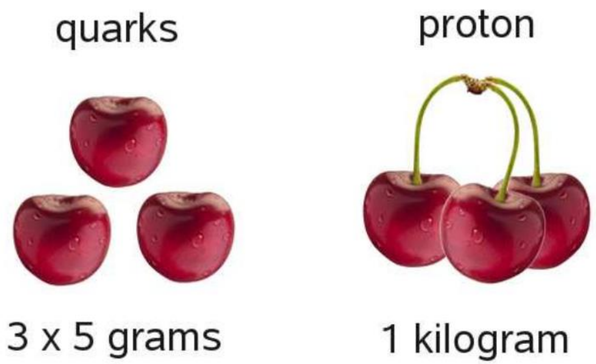

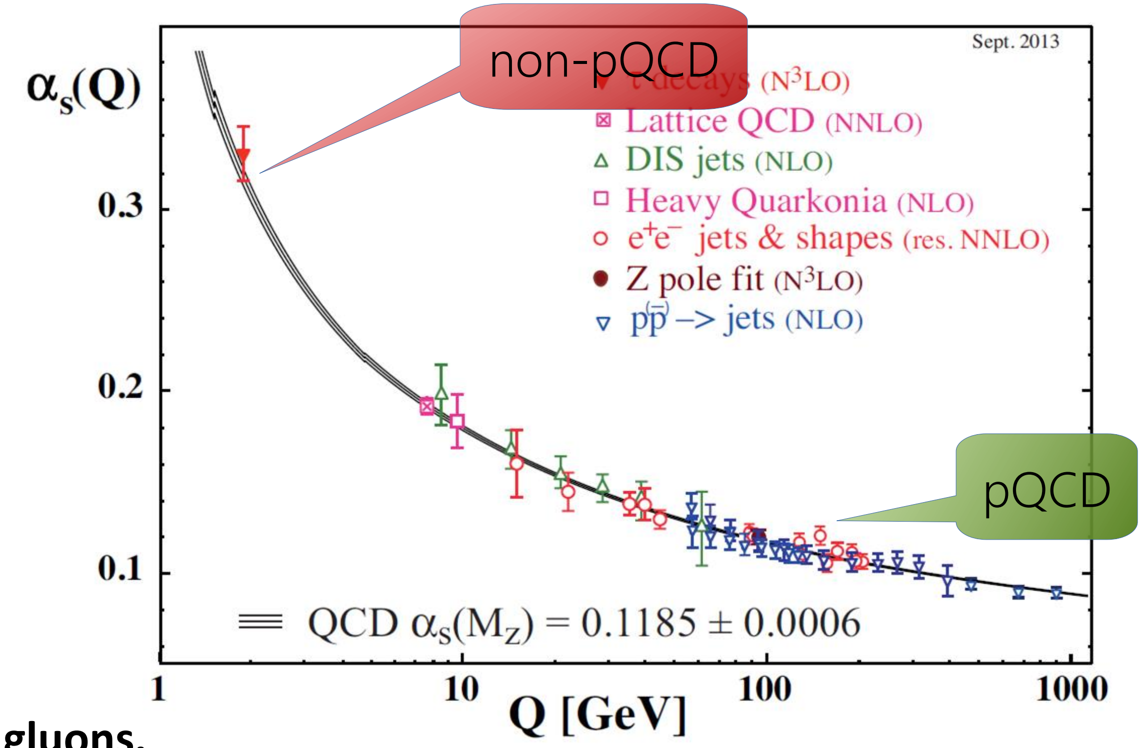

  - the origin of the mass and spin.
  - the mechanism for confinement of quarks and gluons.

- Exploring the internal structure of the nucleon is one path.

Introduction

- **How to explore the internal structure of the nucleon?**
  - **spin of nucleon**
  - **3D structure**
  - **mass of nucleon**
  - **…**

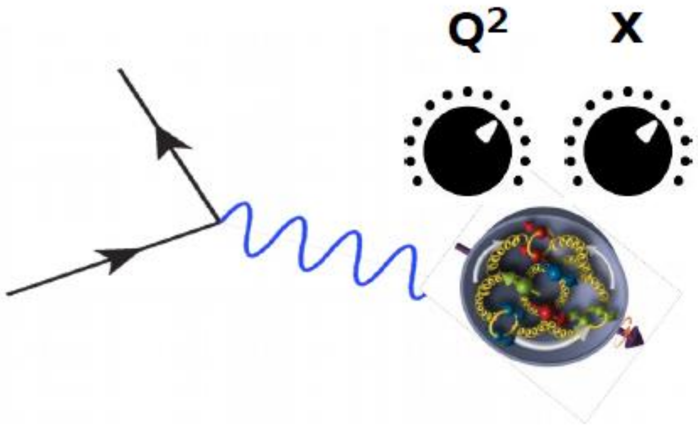

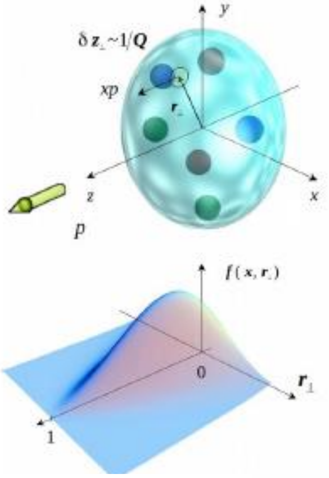

- **Electron Ion Collider (EIC), regarded as a “super electron microscope”, can provide the clearest image inside the nucleon.**

Facilities Landscape

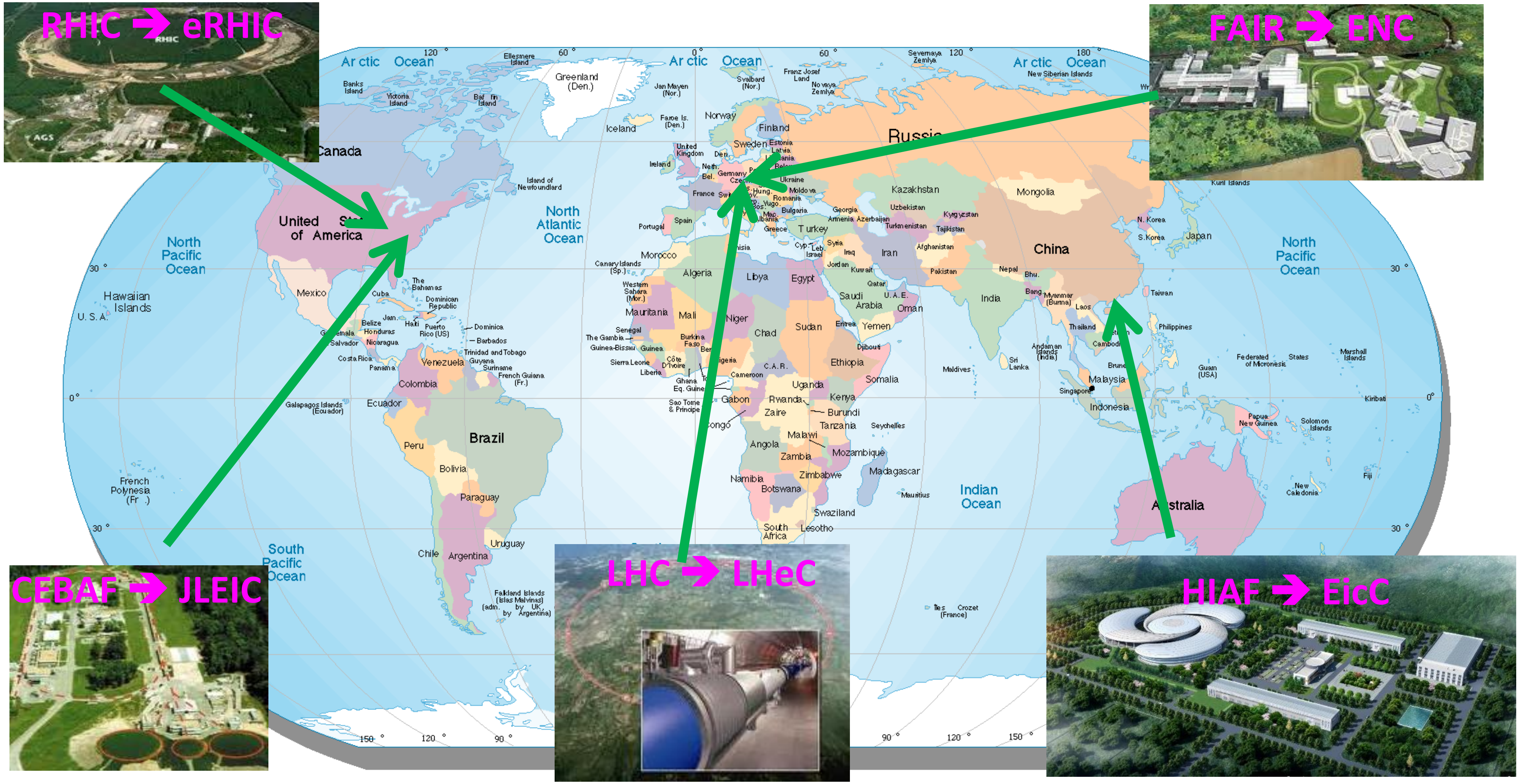

High Intensity heavy-ion Accelerator Facility (HIAF)

Booster Ring:
- Circumference: 569 m
- Rigidity: 34 Tm
- Aacumulation
- Cooling & acceleration

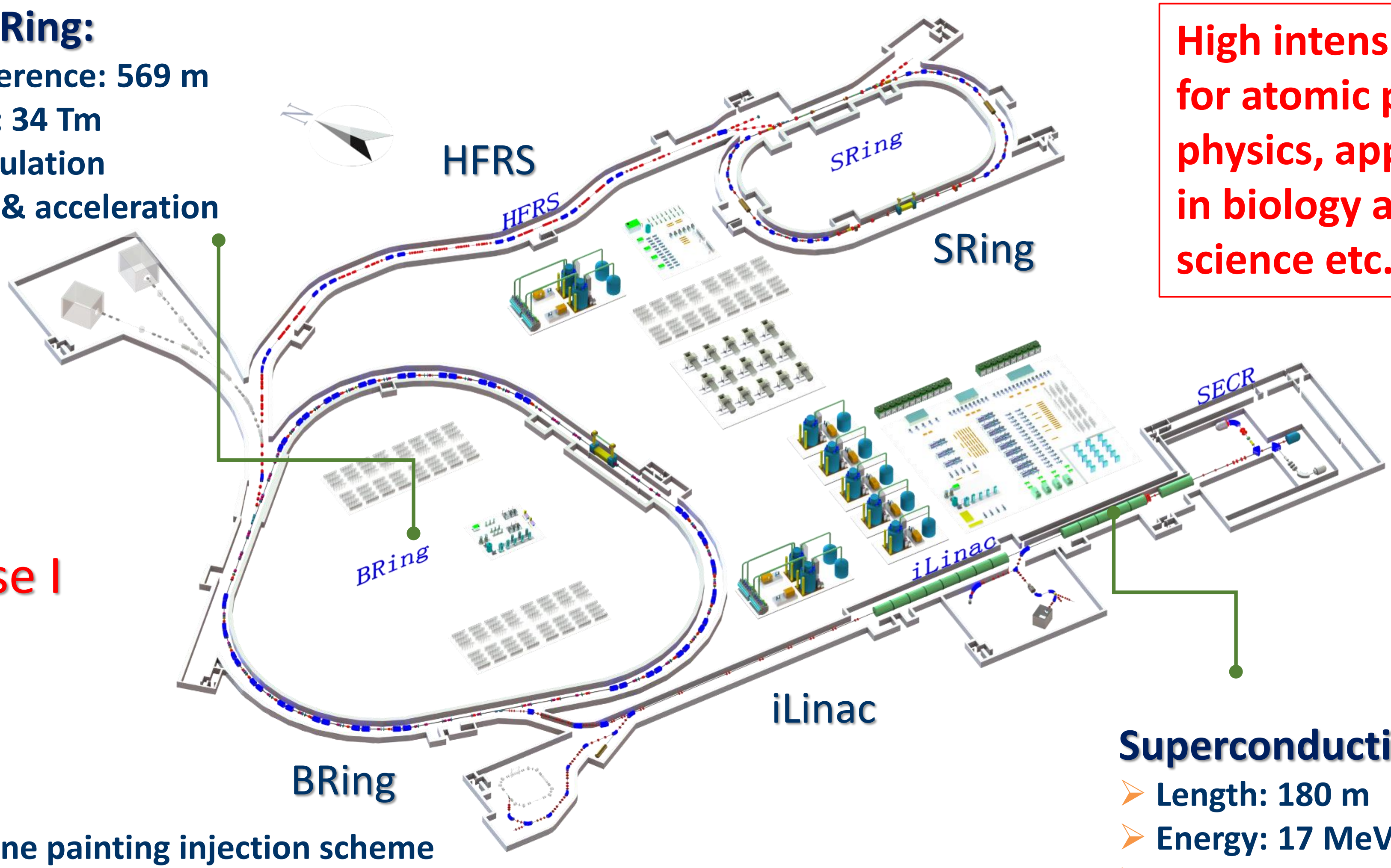

High intensity ion beams for atomic physics, nuclear physics, applied research in biology and material science etc.

Phase I

- Two-plane painting injection scheme
- Fast ramping rate operation

Superconducting Ion Linac:
- Length: 180 m
- Energy: 17 MeV/u (U^{34+})
- CW and pulse modes

EicC accelerator complex overview

- pRing: figure 8
- 2 interaction regions
- 20GeV p + 3.5 GeV e， $\sqrt{S}$=16.7GeV
- High Lumi.： 2-4 x10^{33} cm^{-2}s^{-1}

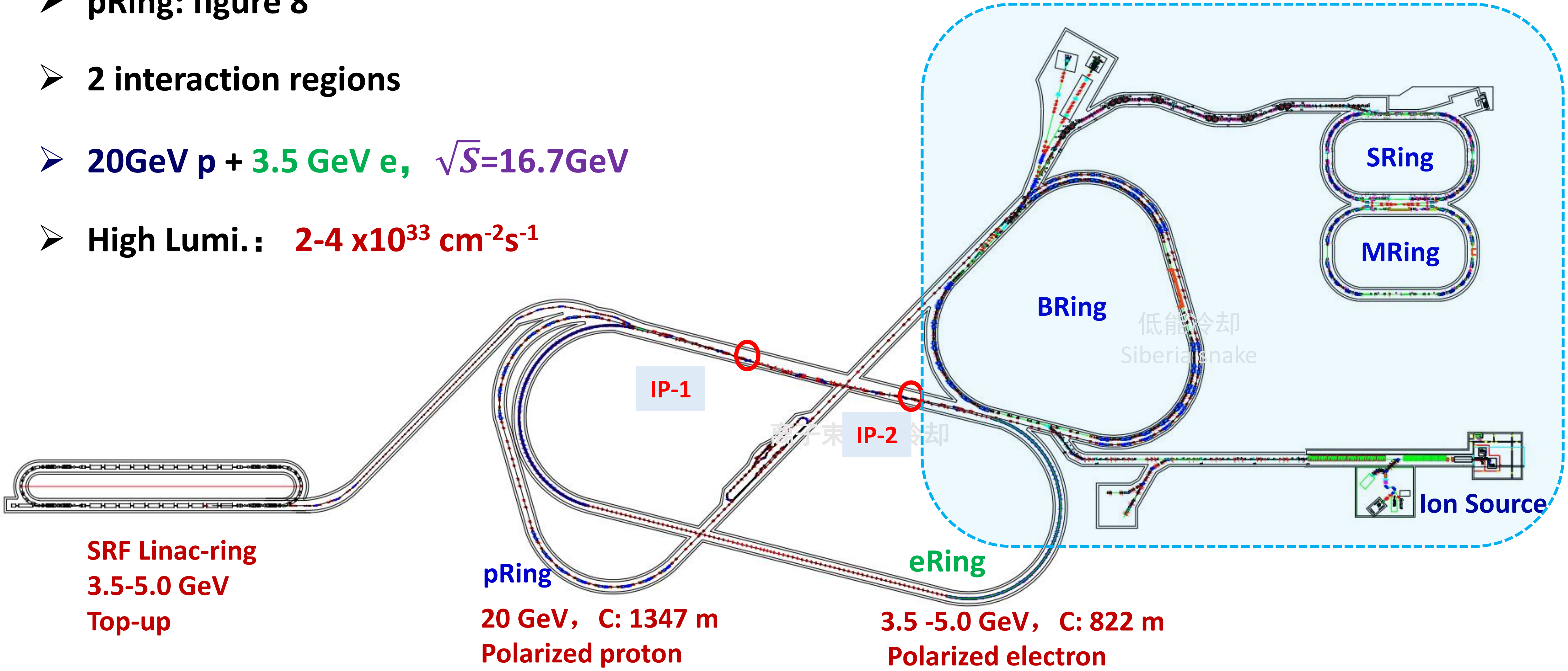

Machine Kinematics

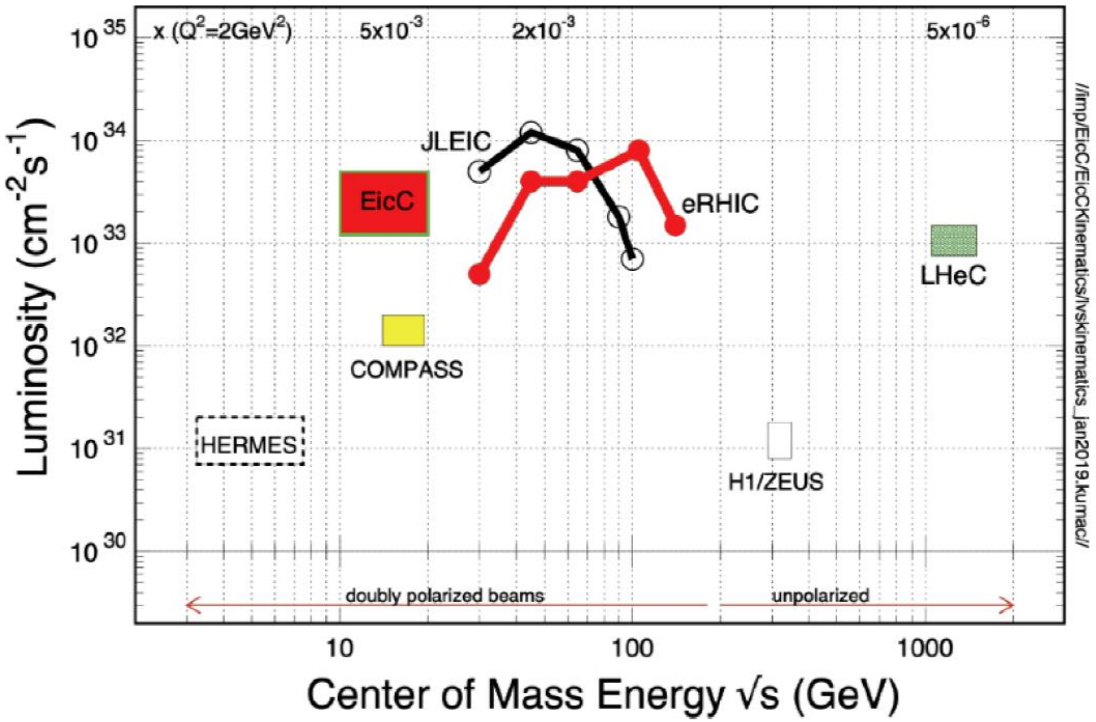

Facilities	Main goals
JLab 12 GeV	Valence quark
EicC	Valence and Sea
US and Europe EIC	gluon

EicC, √s : 15 ~ 20 GeV

- Focus on nuclear physics
- B-quark hadron production

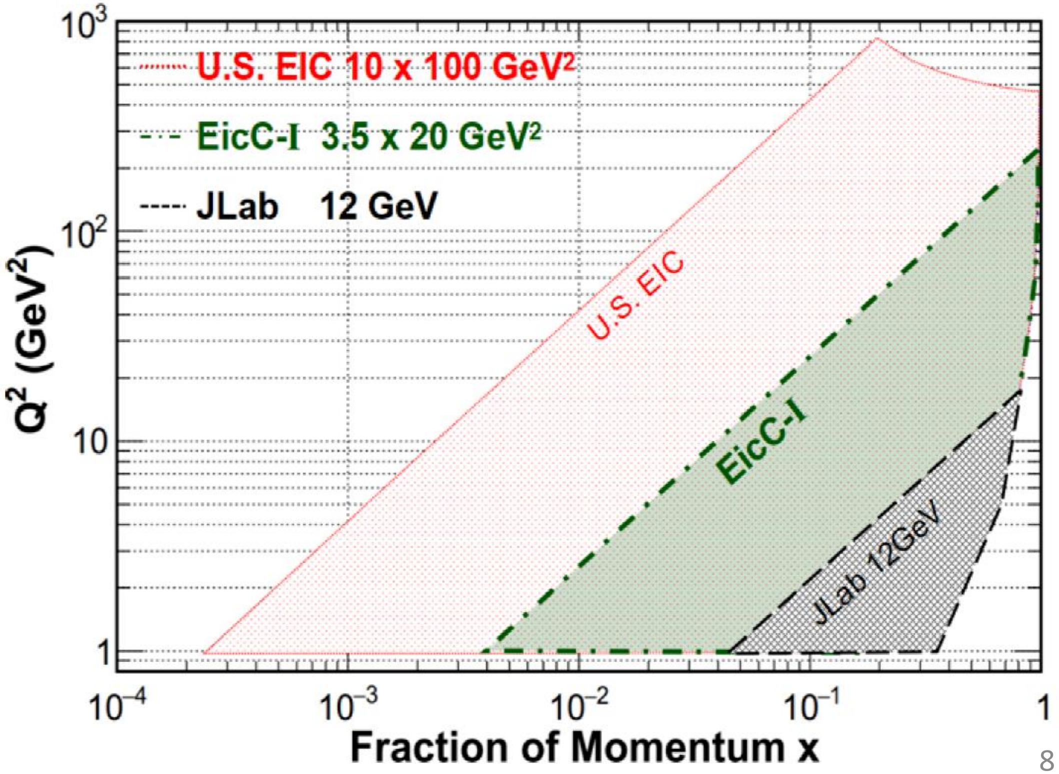

Location of HIAF and EicC

Spin of the Proton

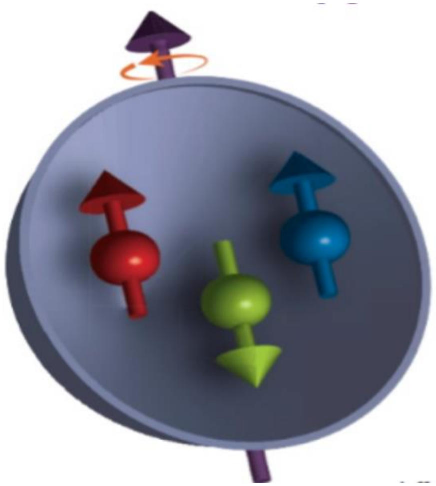

1980s

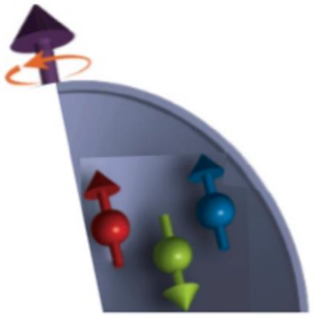

Only ~30% of the proton spin from the quark spin, based on experiments.

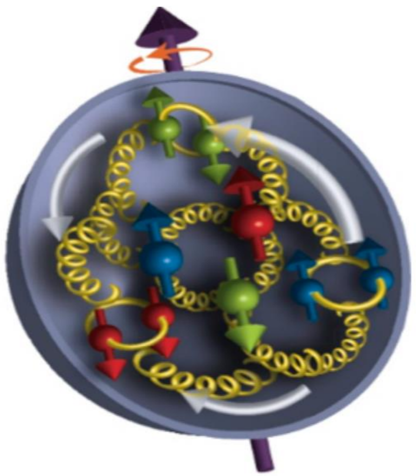

now

$$\frac{1}{2} = S_q + L_q + S_g + L_g$$

$S_q \sim 30\%\, S_p$ [1] $L_q < 70\%\, S_p$ [2,3]

$$S_q(Q^2) = \frac{1}{2}\int_0^1 \Delta\Sigma(x, Q^2)dx \equiv \frac{1}{2}\int_0^1 \left(\Delta u + \Delta\bar{u} + \Delta d + \Delta\bar{d} + \Delta s + \Delta\bar{s}\right)(x, Q^2)dx$$

[1] EMC, J. Ashman et al., Phys. Lett. B206, 364 (1988).
[2] Lattice: P. Hagler, Phys. Rept. 490, 49 (2010)
[3] Lattice: Yi-Bo Yang, R. Sufian, et. A., PRL118, 042001(2017)
[4] EPJA52, 268 (2016), arXiv: 1212.1701
[5] D. Florian, PRL 113, 012001 (2014)
[6] STAR NPA932, 500(2014),1404.5134
[7] PHENIX PRD90, 012007(2014), 1402.6296
[8] COMPASS PLB690, 466(2010), 1001.4654
[9] X. Ji, J. Zhang, and Y. Zhao, PRL111 112002 (2013)

The Longitudinal Spin of the Nucleon

$$\frac{1}{2} = S_q + L_q + S_g + L_g$$

$$\frac{1}{2}\left[\frac{d^2\sigma^{\rightleftarrows}}{dx\, dQ^2} - \frac{d^2\sigma^{\rightrightarrows}}{dx\, dQ^2}\right] \simeq \frac{4\pi\,\alpha^2}{Q^4} y\,(2-y)\, g_1(x, Q^2)$$

$$g_1(x, Q^2) = \frac{1}{2}\sum e_q^2 \left[\Delta q(x, Q^2) + \Delta\bar{q}(x, Q^2)\right]$$

EicC projection with 50 fb^{-1} lumi.

- **Improving in the low x region**
- **High luminosity and large acceptance.**

Plot Courtesy of Yuxiang Zhao

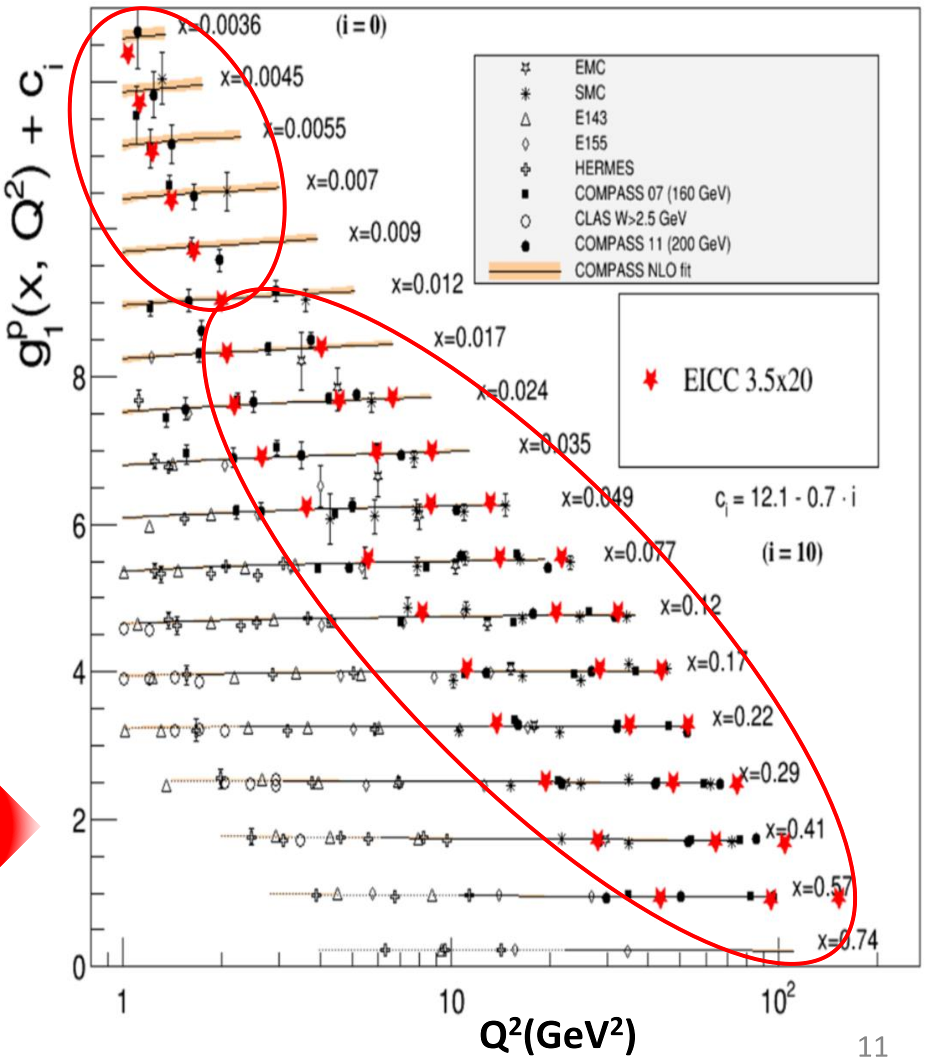

The Longitudinal Spin of the Nucleon

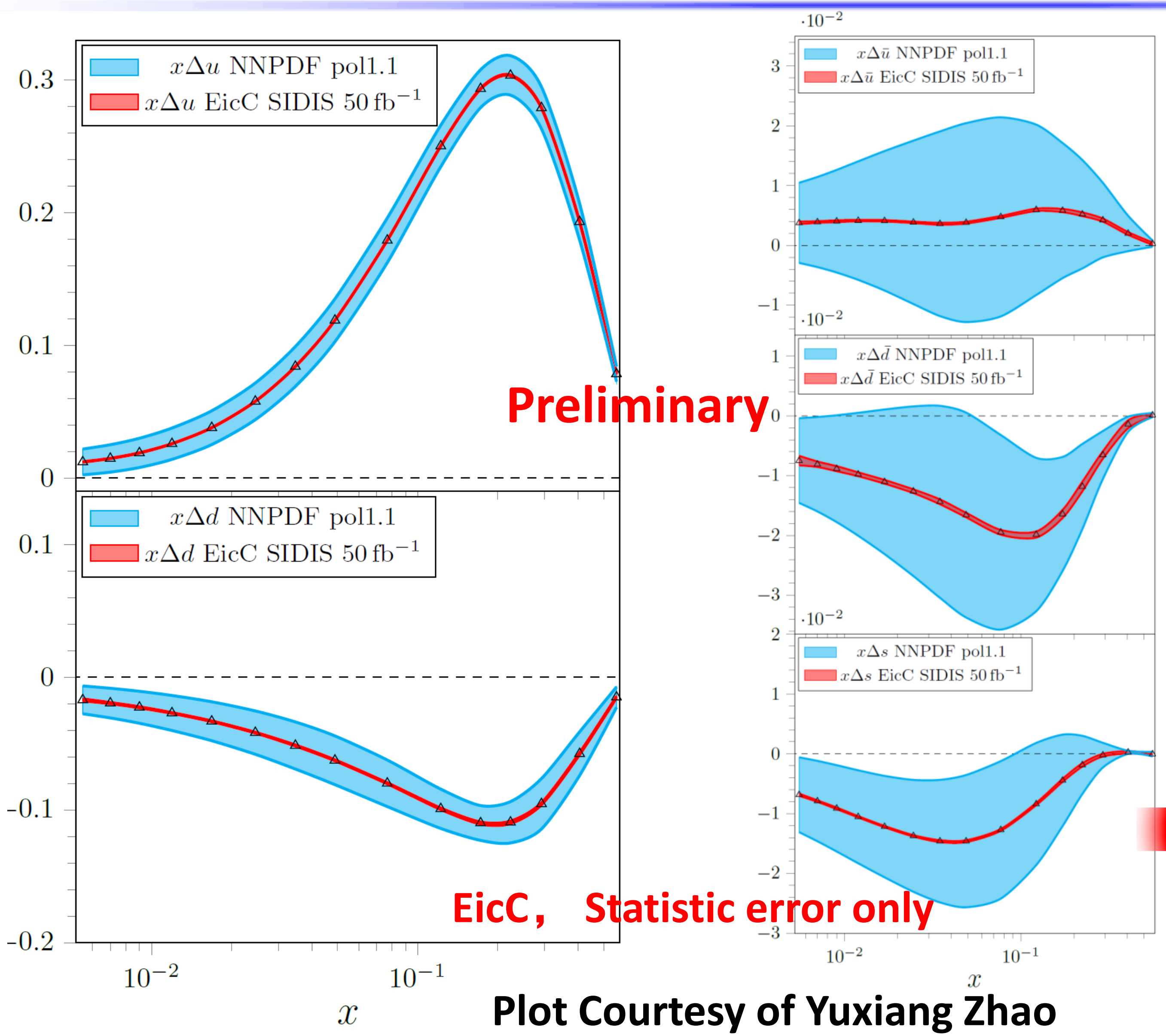

EicC SIDS data:

- Pion(+/-), Kaon(+/-)
- ep: 3.5 GeV X 20 GeV
- eHe-3: 3.5 GeV X 40 GeV
- Pol.: e(80%), p(70%),
  He-3(70%)
- Lumi: ep 50 fb^{-1}
  eHe-3 50 fb^{-1}

EicC, precise measurements, especially in sea quark region.

Plot Courtesy of Yuxiang Zhao

Fragmentation function used: DSS

3D Structure of Nucleons – TMDs & GPDs

In Quantum Dynamics, a known particle's full state is $\psi(\vec{x}, \vec{k}, t)$. In particle physics, the spatial dimension along the energy transfer direction (i.e., Z-axis) is ignored due to the relativistic effect. Also at t=0, it is a 5D space.

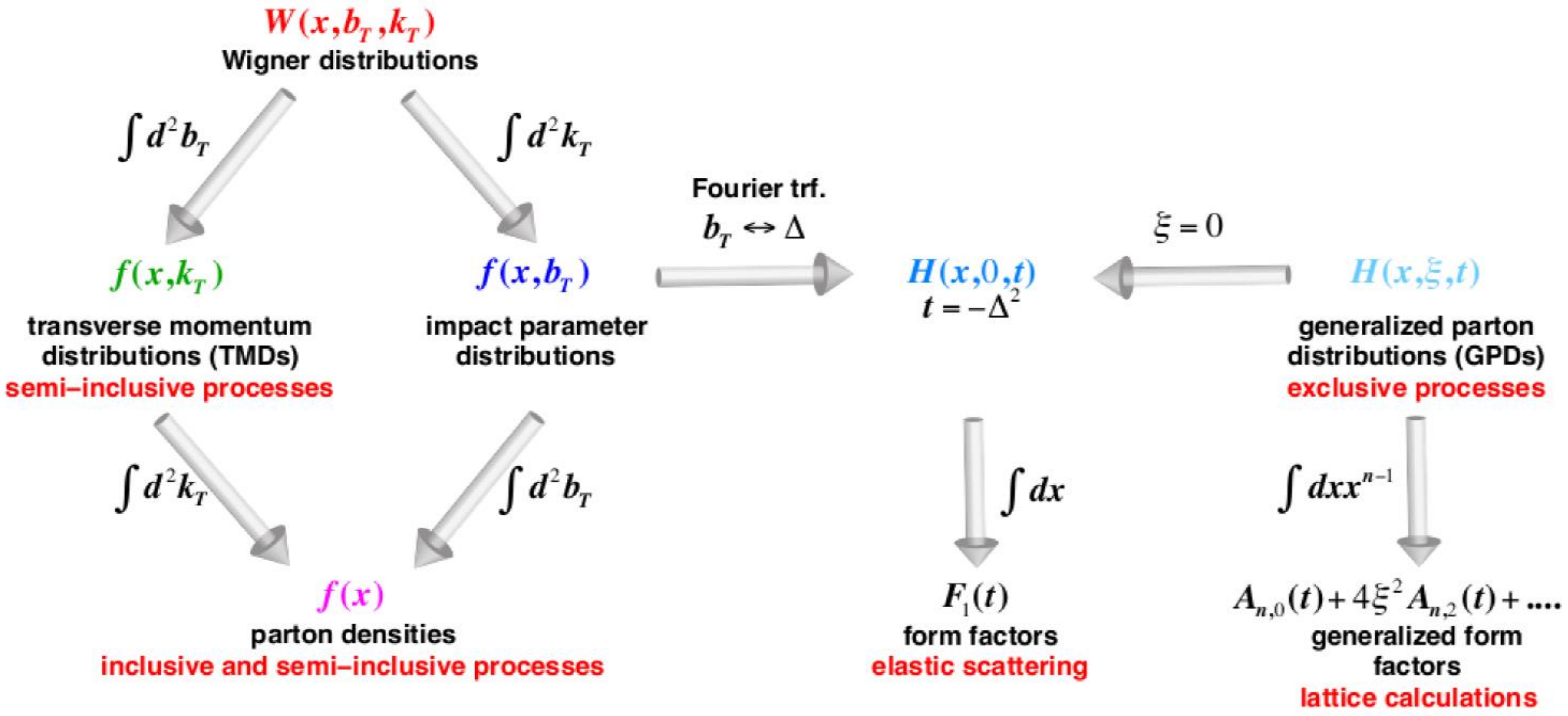

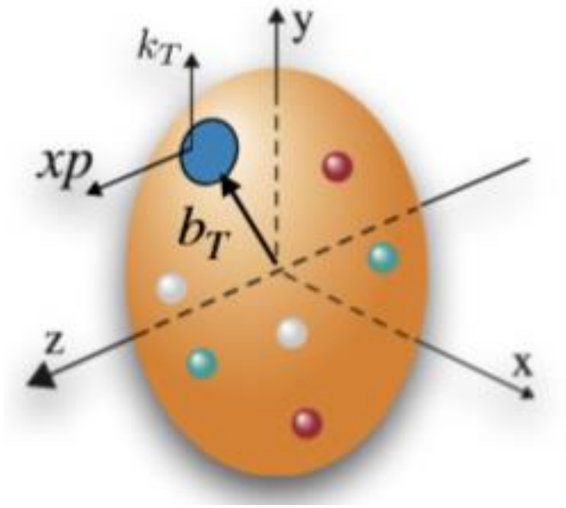

TMD =
1D Longitudinally Momentum
+ 2D Transverse Momentum

GPD =
1D Longitudinally Momentum
+ 2D Transverse Position

Transverse Momentum Dependent Functions (TMDs)

Unpolarized Density Function:

$$f_1(x) = \int d^2\boldsymbol{k}_\perp \, f_1(x, k_\perp)$$

Helicity Function:

$$g_1(x) = \int d^2\boldsymbol{k}_\perp \, g_{1L}(x, k_\perp)$$

Transversity Function:

$$h_1(x) = \int d^2\boldsymbol{k}_\perp \, [h_{1T}(x, k_\perp) + \frac{k_\perp^2}{2M^2} h_{1T}^\perp(x, k_\perp)]$$

		Quark Polarization		
		U	L	T
Nucleon Polarization	U	f_1 unpolarized		$h_1^\perp$ Boer-Mulders
	L		g_{1L} helicity	$h_{1L}^\perp$ longi-transversity (worm-gear)
	T	$f_{1T}^\perp$ Sivers	g_{1T} trans-helicity (worm-gear)	h_1 transversity $h_{1T}^\perp$ pretzelosity

Nucleon spin Quark spin

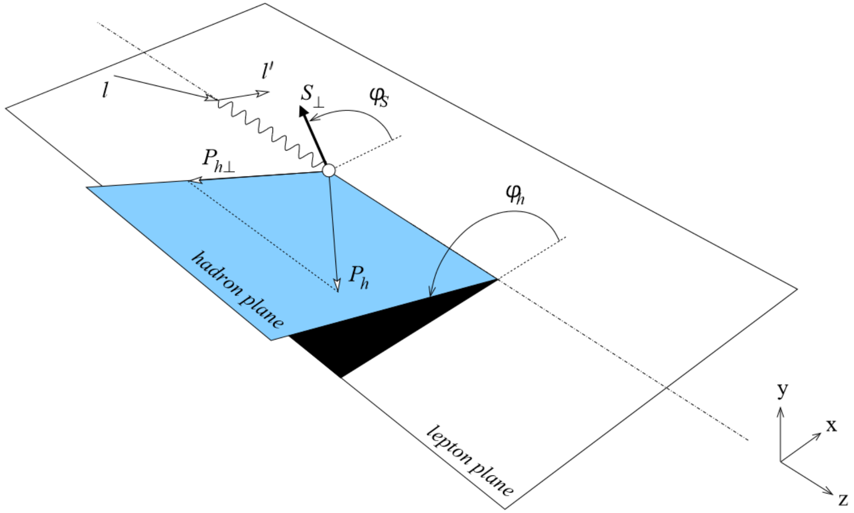

$$\frac{d\sigma}{dx\,dy\,dz\,dP_{hT}^2\,d\varphi_h\,d\psi} = \left[\frac{\alpha}{xyQ^2}\frac{y^2}{2(1-\varepsilon)}\left(1+\frac{\gamma^2}{2x}\right)\right] \times \left(F_{UU,T} + \varepsilon F_{UU,L}\right) \times$$

$$\left\{1 + \cos\varphi_h \times \sqrt{2\varepsilon(1+\varepsilon)}A_{UU}^{\cos\varphi_h} + \cos(2\varphi_h) \times \varepsilon A_{UU}^{\cos(2\varphi_h)} + \right.$$

$$\left. \lambda \sin\varphi_h \times \sqrt{2\varepsilon(1-\varepsilon)}A_{LU}^{\sin\varphi_h} + \right.$$

Asymmetries → TMDs

A.Kotzinian, Nucl. Phys. **B441**, 234 (1995). *Bacchetta, Diehl, Goeke, Metz, Mulders and Schlegel* JHEP 0702:093 (2007)

SIDIS Observables

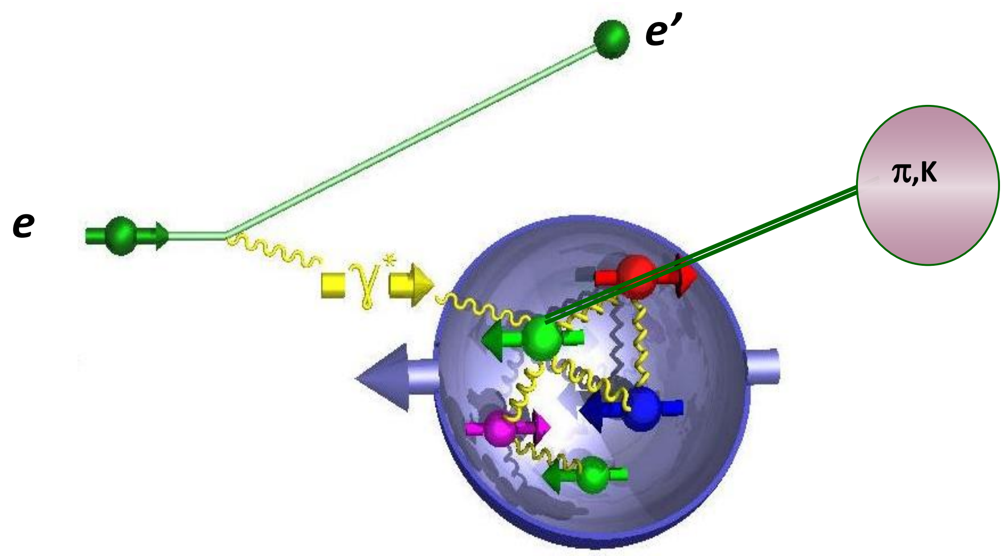

SIDIS: Detect scattered electrons and produced single-hadron in the final state.

Measuring different hadrons, as flavor-tagger to probe the internal quark structure of nucleons.

- perform multidimensional analyses to disentangle all the relevant kinematical dependencies
- provide hadron identification to access the parton flavor
- large and uniform acceptance
- with high luminosity.

EicC projections on Sivers

u/d Sivers EicC vs world data

LO analysis

EicC SIDS data:

- Pion(+/-), Kaon(+/-)
- ep: 3.5 GeV X 20 GeV
- eHe-3: 3.5 GeV X 40 GeV
- Pol.: e(80%), p(70%), He-3(70%)
- Lumi: ep 50 fb^{-1}, eHe-3 50 fb^{-1}

EicC, precise measurements, especially in sea quark region.

Preliminary

Plot Courtesy of Tianbo Liu

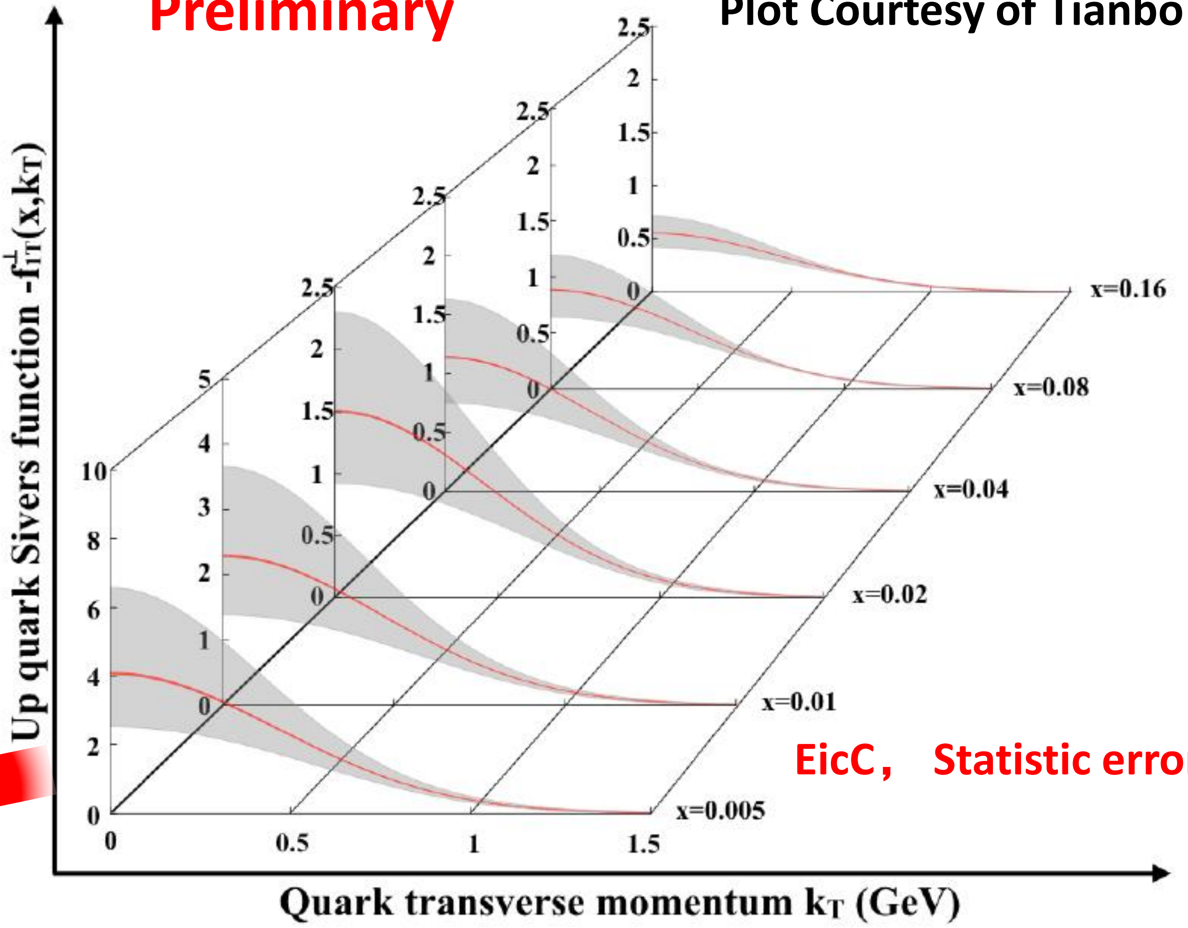

EicC， Statistic error only

Generalized Parton Distributions (GPDs)

Eight GPDs for quarks or gluons

		Quark Polarization		
		Unpolarized (U)	Longitudinally Polarized (L)	Transversely Polarized (T)
Nucleon Polarization	U	H		$2\widetilde{H}_T + E_T$
	L		$\widetilde{H}$	$\widetilde{E}_T$
	T	E	$\widetilde{E}$	$H_T, \widetilde{H}_T$

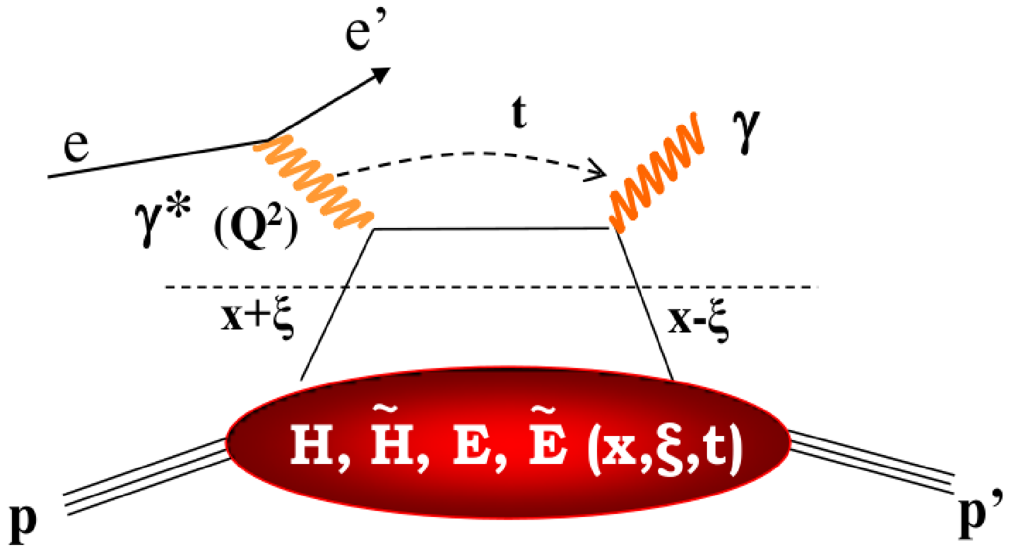

- **GPDs encode information about the spatial distribution of partons inside a hadron, correlated with their distribution in longitudinal momentum.**
- **GPD is related to quark angular momentum.**

Ji's sum rule [1] $$J^f(Q^2) = \frac{1}{2} \lim_{t\to 0} \int_{-1}^{1} \mathrm{d}x \; x \; \left[H^f(x,\xi,t,Q^2) + E^f(x,\xi,t,Q^2)\right],$$

- **Exclusive reactions, such as DVCS or DVMP, can get access to GPDs.**

[1] X.-D. Ji, Phys. Rev. Lett. 78 (1997) 610.

Probe GPD via DVCS

- **Detect the scattered electron, real photon and nucleon.**

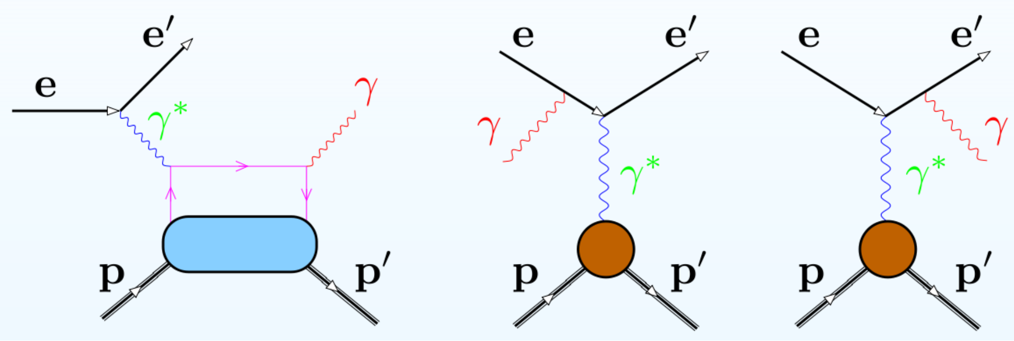

- **Absolute Cross Section:**

$$\frac{d\sigma}{dQ^2 dx_B dt d\phi} \propto |\tau_{DVCS}|^2 + I + |\tau_{BH}|^2$$

$$\tau_{DVCS} \propto \int_{-1}^{+1} \frac{H(x,\xi,t)}{x \pm \xi \mp i\varepsilon} dx = P\int_{-1}^{+1} \frac{H(x,\xi,t)}{x \pm \xi} dx - i\pi H(\pm\xi,\xi,t),$$

- **Asymmetries with polarized target and/or polarized beam:**

$$A = \frac{I}{|\tau_{DVCS}|^2 + I + |\tau_{BH}|^2} = \frac{\sigma^+ - \sigma^-}{\sigma^+ + \sigma^-}$$

$\sigma^{+/-}$: Beam or/and Target Polarization.

Polarization	Asymmetries	CFFs
Longitudinal Beam	A_{LU}	$Im\{\mathcal{H}_p, \widetilde{\mathcal{H}}_p, \mathcal{E}_p\}$ $Im\{\mathcal{H}_n, \widetilde{\mathcal{H}}_n, \mathcal{E}_n\}$
Longitudinal Target	A_{UL}	$Im\{\mathcal{H}_p, \widetilde{\mathcal{H}}_p,\}$ $Im\{\mathcal{H}_n, \mathcal{E}_n, \widetilde{\mathcal{E}}_n\}$
Long. Beam + Long. Target	A_{LL}	$Re\{\mathcal{H}_p, \widetilde{\mathcal{H}}_p,\}$ $Re\{\mathcal{H}_n, \mathcal{E}_n, \widetilde{\mathcal{E}}_n\}$
Transverse Target	A_{UT}	$Im\{\mathcal{H}_p, \mathcal{E}_p\}$ $Im\{\mathcal{H}_n\}$
Long. Beam +Trans.Targt	A_{LT}	$Re\{\mathcal{H}_p, \mathcal{E}_p\}$ $Re\{\mathcal{H}_n\}$

GPD -- EicC Projections

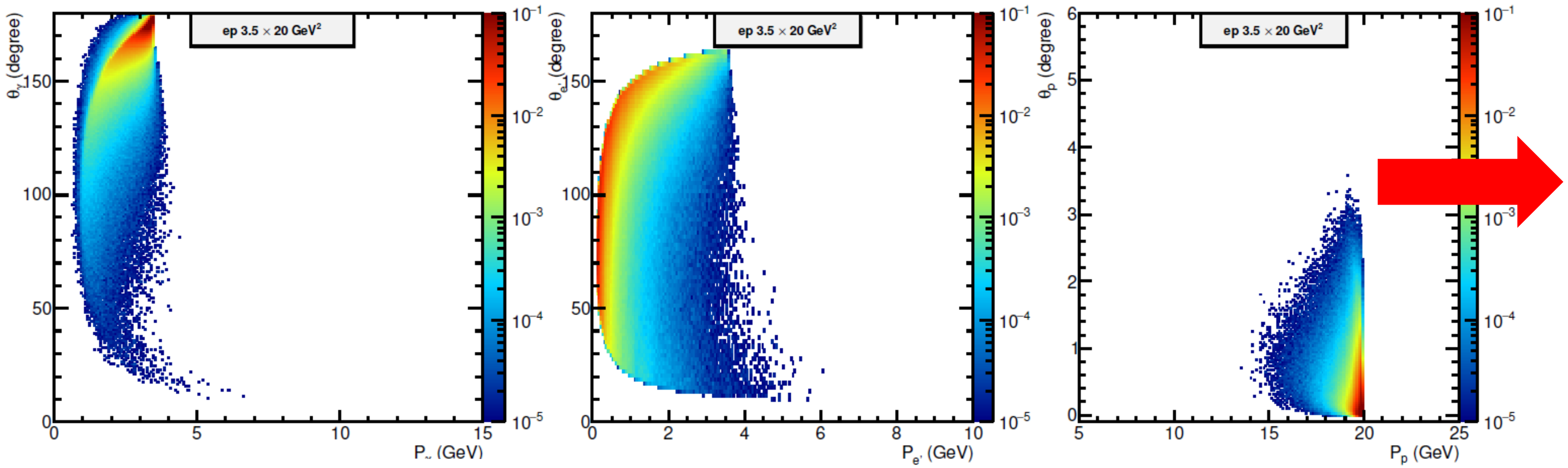

Need far-forward detection of scattered proton.

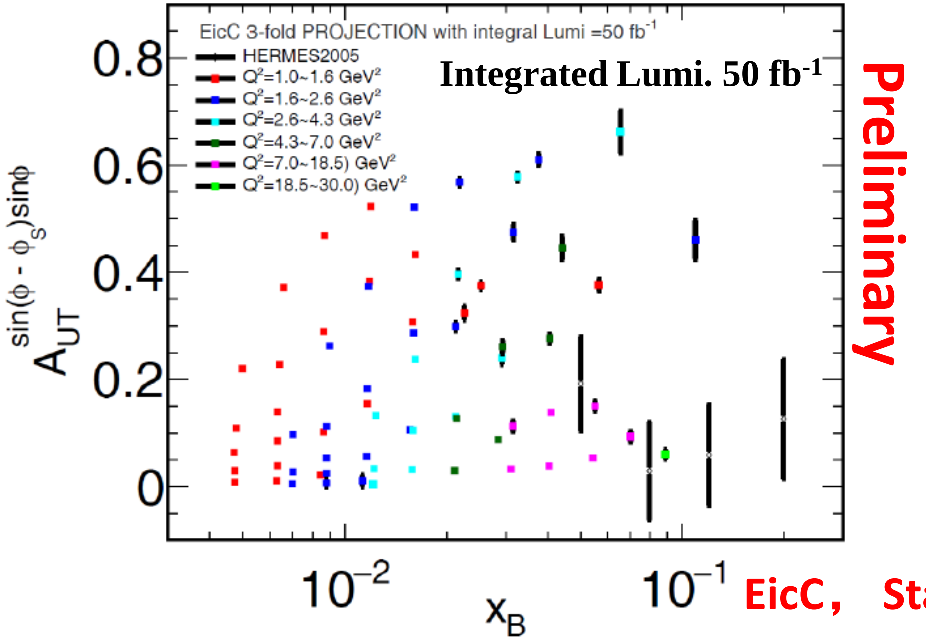

EicC， Statistic error only

Plot Courtesy of Qiang Fu and Xu Cao.

EicC can measure GPD related asymmetries:
- In high precision
- In multi-dimensional bins
- on p and n for flavor separations

Proton Mass

Proton mass decomposition[1]:

$$\widetilde{M}_q = \frac{\langle P|H_q|P\rangle}{\langle P|P\rangle} = \frac{3}{4}\left(a - \frac{b}{1+\gamma_m}\right)M,$$

$$\widetilde{M}_g = \frac{\langle P|H_g|P\rangle}{\langle P|P\rangle} = \frac{3(1-a)}{4}M,$$

$$\widetilde{M}_m = \frac{\langle P|H_m|P\rangle}{\langle P|P\rangle} = \frac{b}{4}\frac{4+\gamma_m}{1+\gamma_m}M,$$

$$\widetilde{M}_a = \frac{\langle P|H_a|P\rangle}{\langle P|P\rangle} = \frac{1-b}{4}M.$$

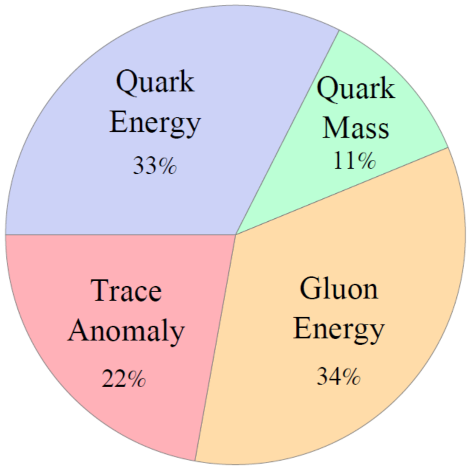

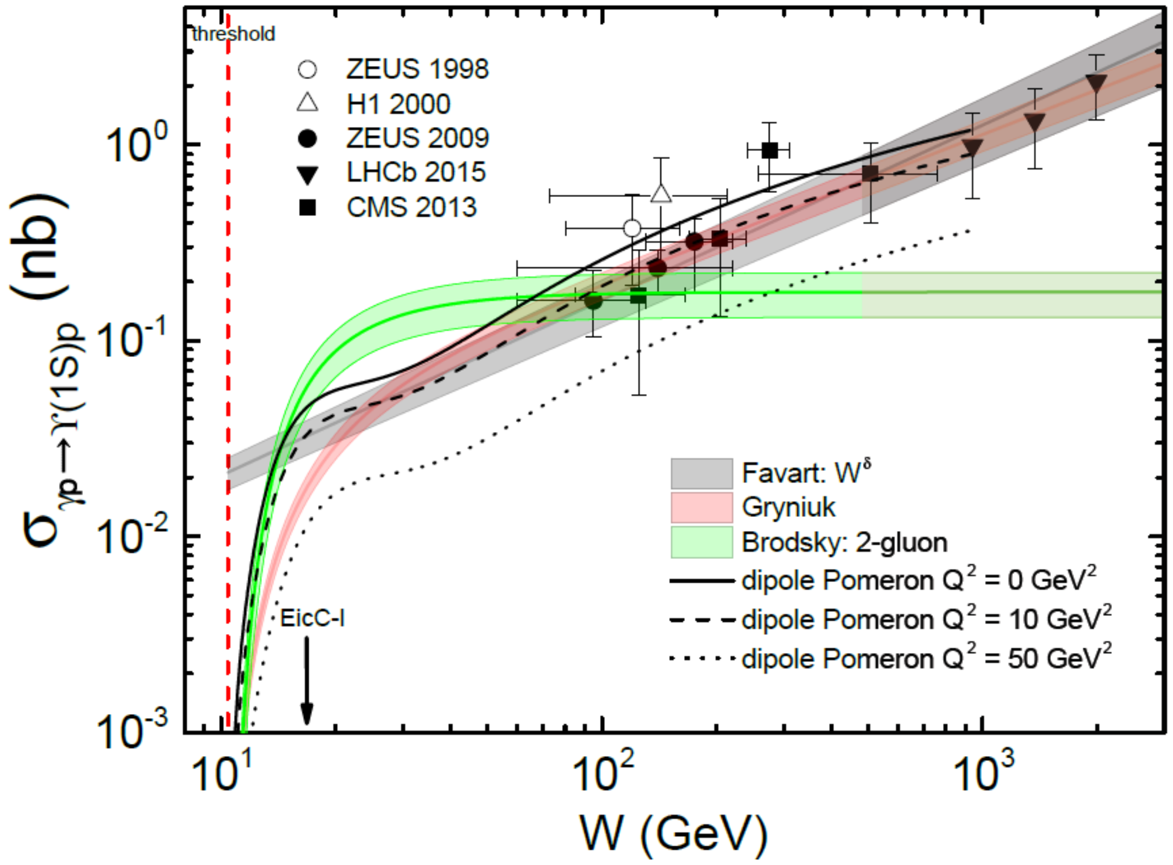

a: **related to PDFs, well constrained**

b: **related to quarkonium-proton scattering amplitude $M_{\psi p}$ near-threshold**

[1] X. Ji, PRL 74, 1071 (1995) & PRD 52, 271 (1995)

Other interesting topics

- Pion/Kaon structure
- Hadronization
- Hadron Spectroscopy
- And more…

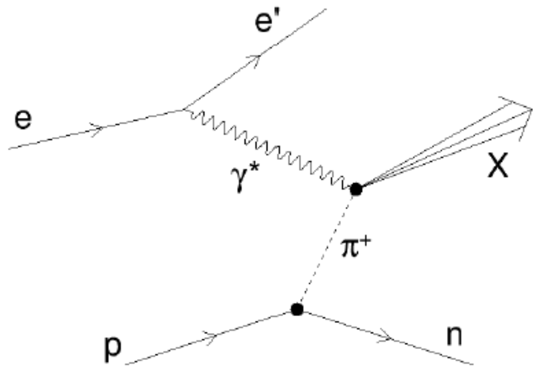

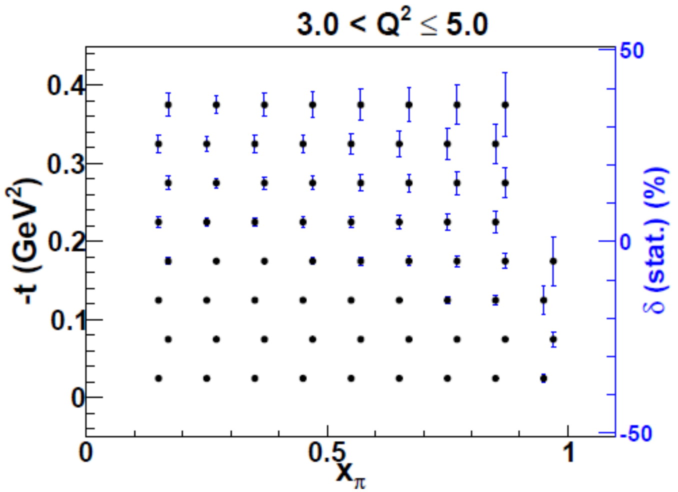

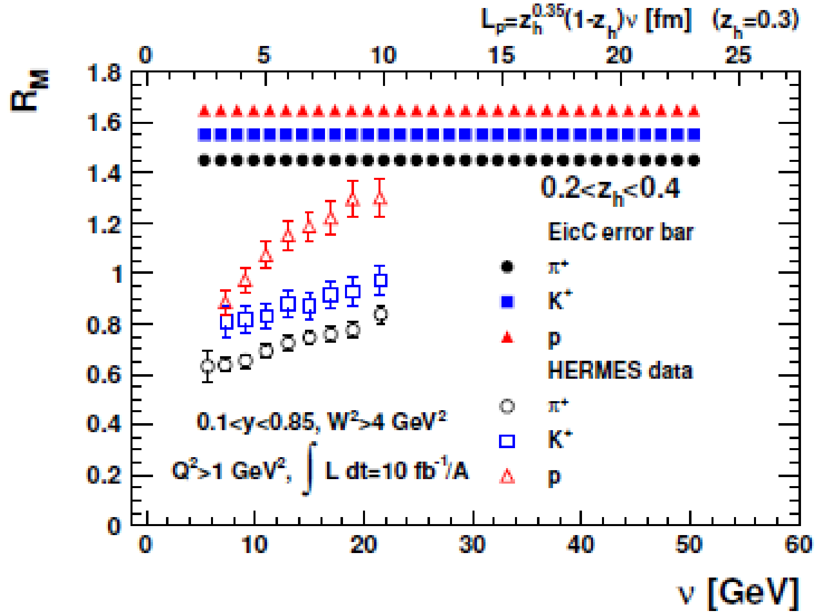

EicC detector conceptual design

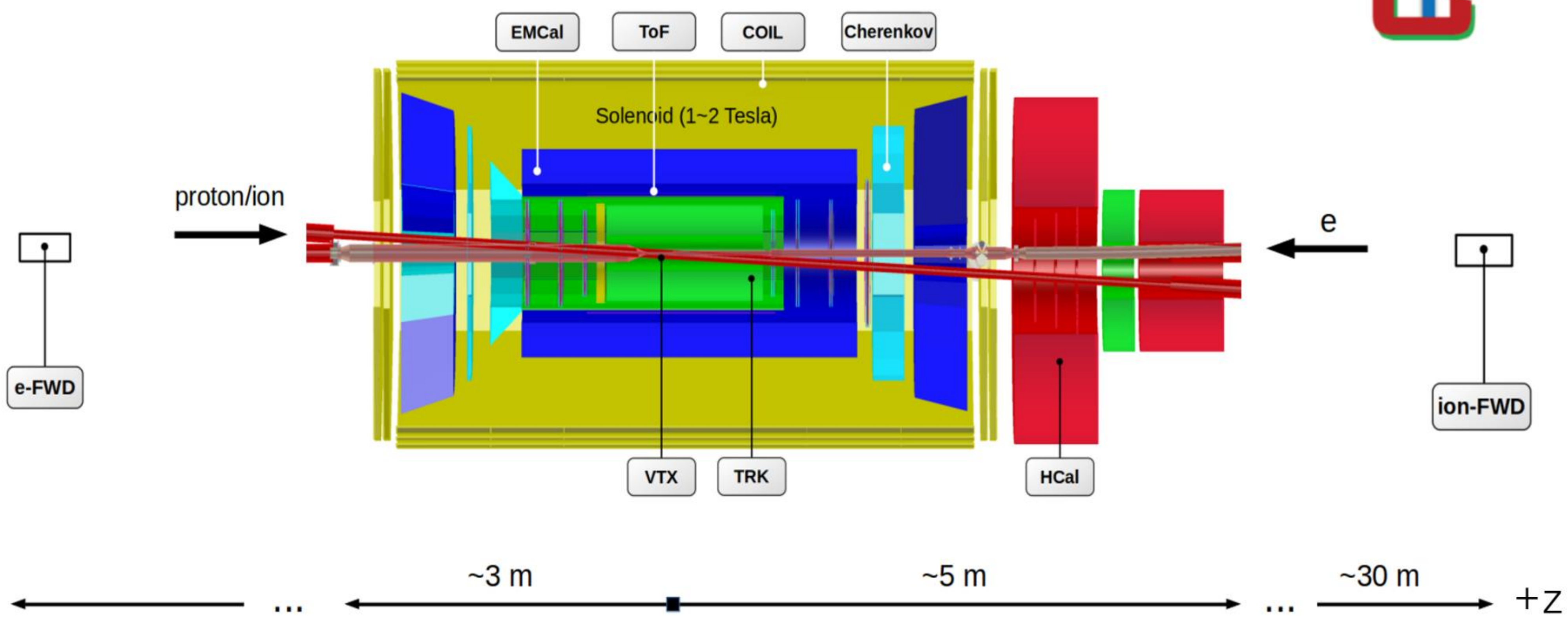

Very first design; detector options are open.

EicC Status

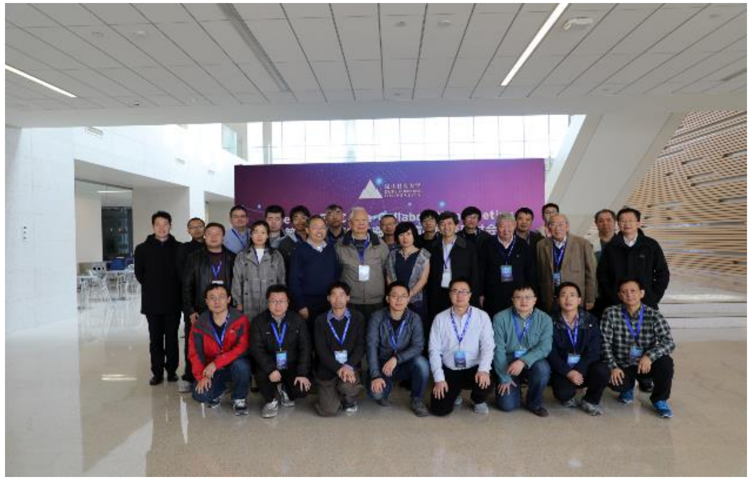

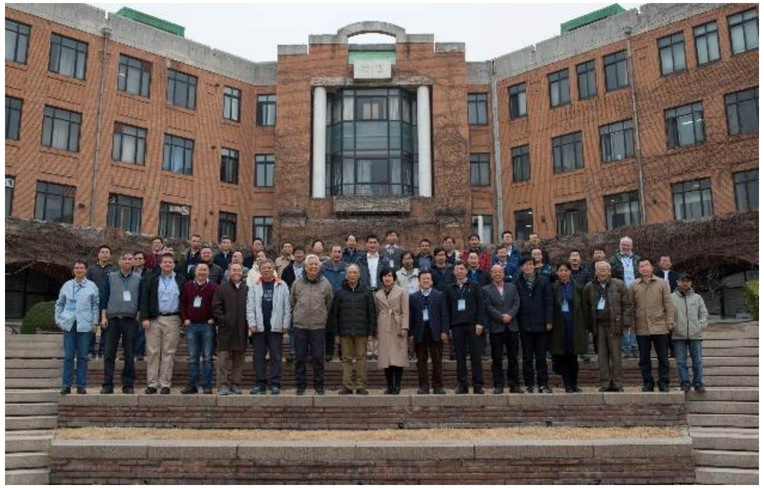

4 pre-Collaboration meetings up to now.

Discussions on:
physics programs,
simulations
accelerator, detector.

EicC white paper

1. Chinese Version by the end of 2019,
2. English Version by the middle of 2020.

Electron Ion Collider in China

Yutie Liang(梁羽铁)
Institute of Modern Physics, CAS
中科院近代物理研究所

Summary

- EicC has been proposed based on the HIAF facility.

  -- polarized electron beam (3.5 GeV)

  -- polarized proton beam (20 GeV)/ion beam (20 GeV/u)

- High precision measurements for 1D (helicity), 3D (TMDs/GPDs) nucleon structure study with flavor separation in the valence and sea quark dominated region.

- Other interesting physics topics will be delivered as well, not mentioned here in details.

Welcome to join us! **EicC@impcas.ac.cn**

Thank You

EicC detector requirements

Detector segments

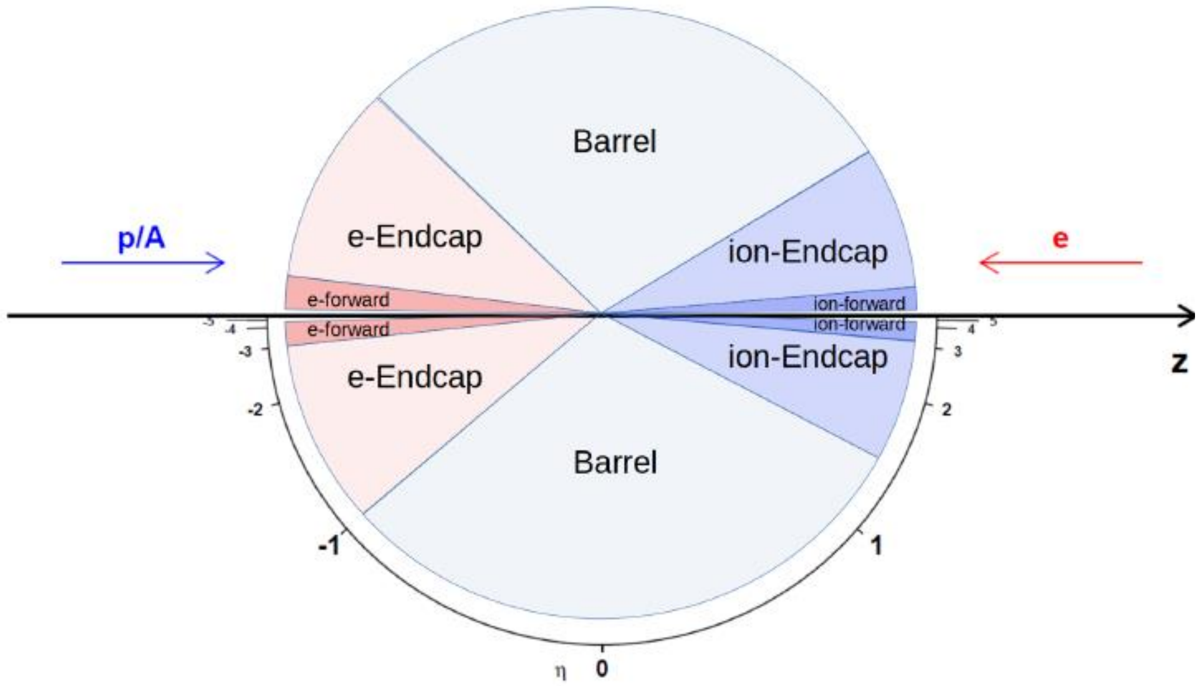

Interaction rate and multiplicity

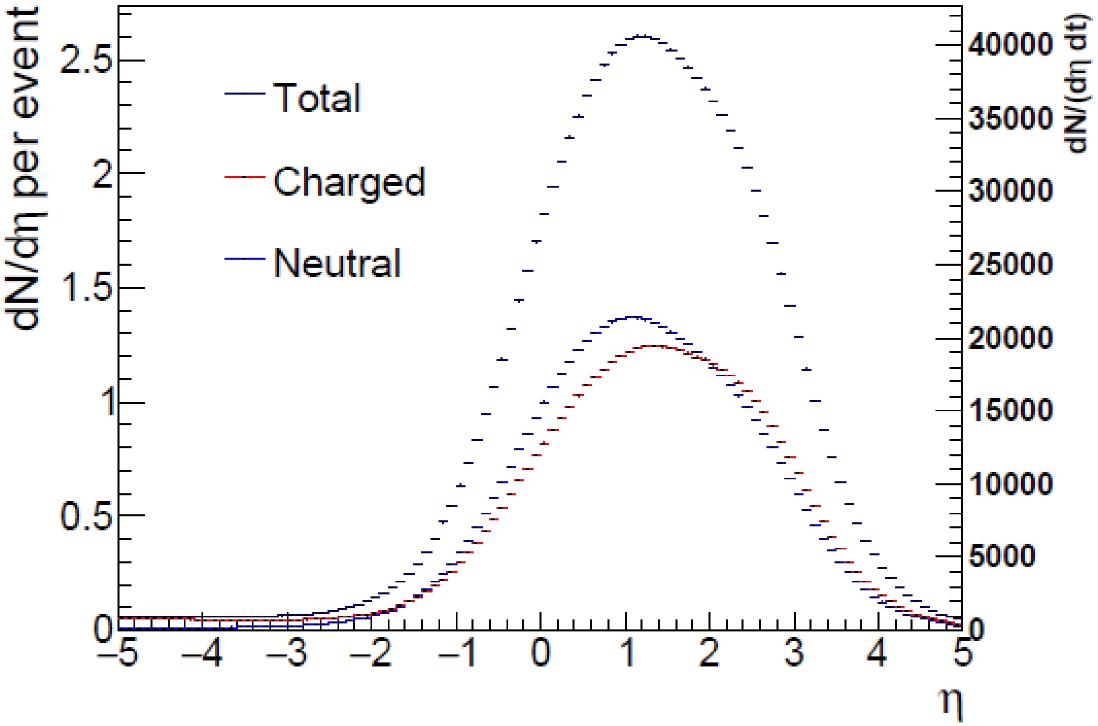

- **20 ~ 40 KHz**
- **~ 8 charged + ~ 8 neutrals**

Scattering electron distributions

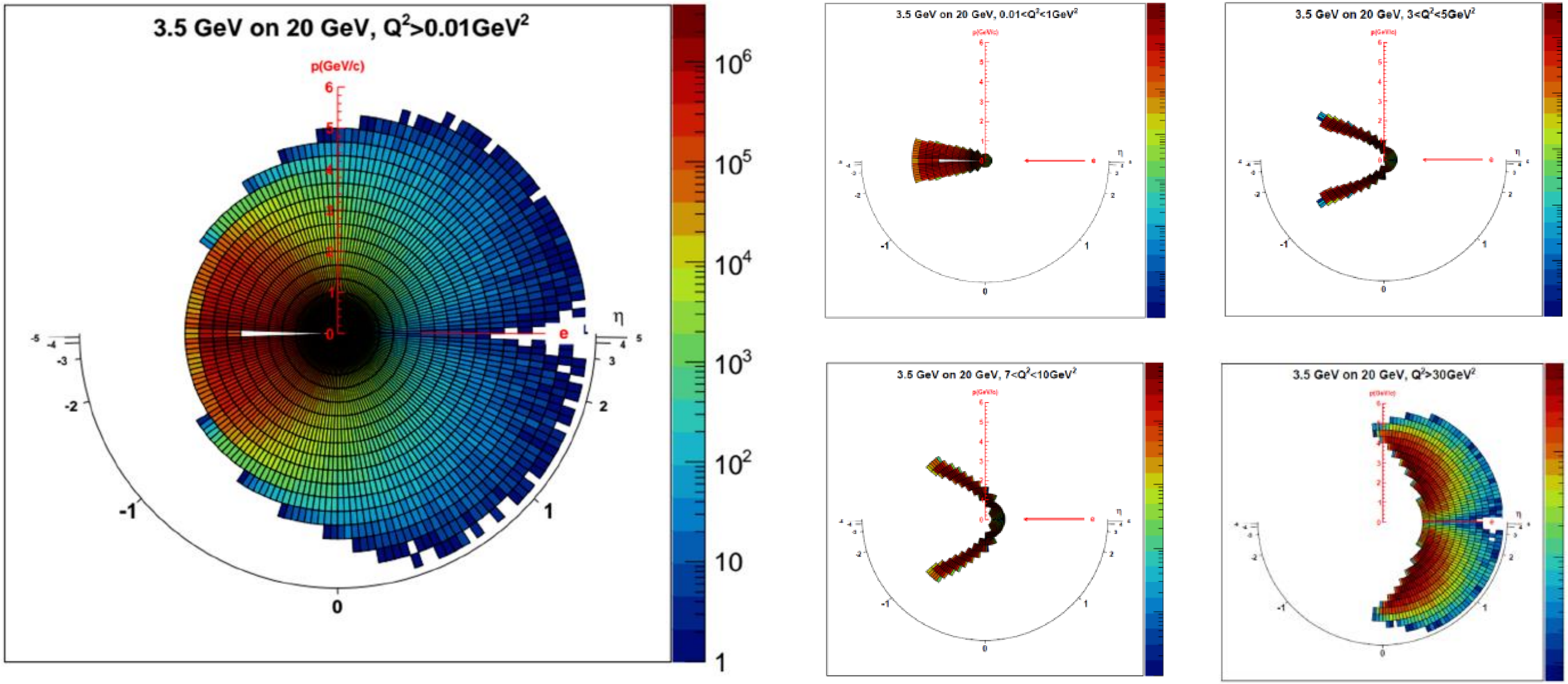

Final state hadrons

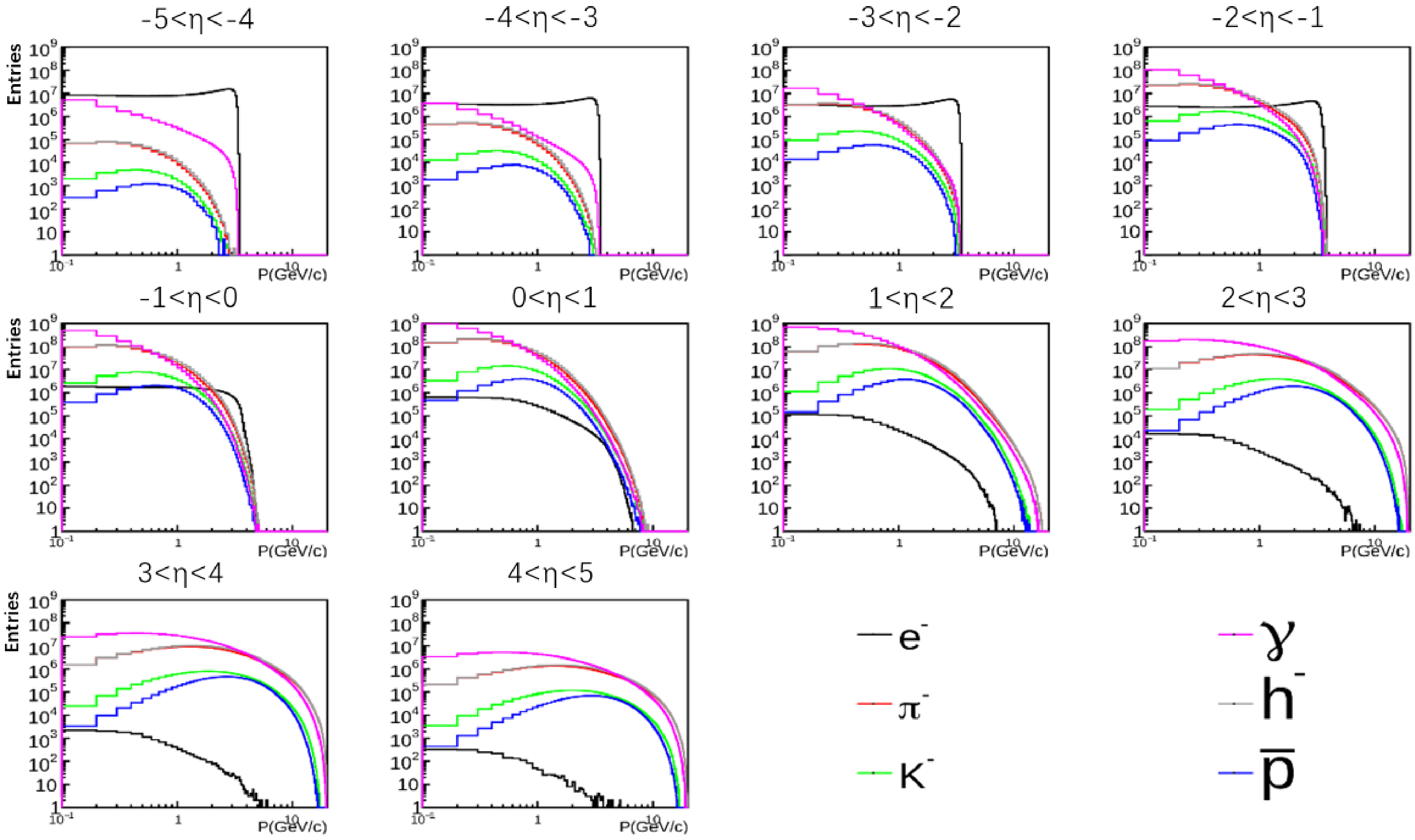

EicC detector requirements

SIDIS: very general requirement.

DVCS: detection of proton at forward direction.

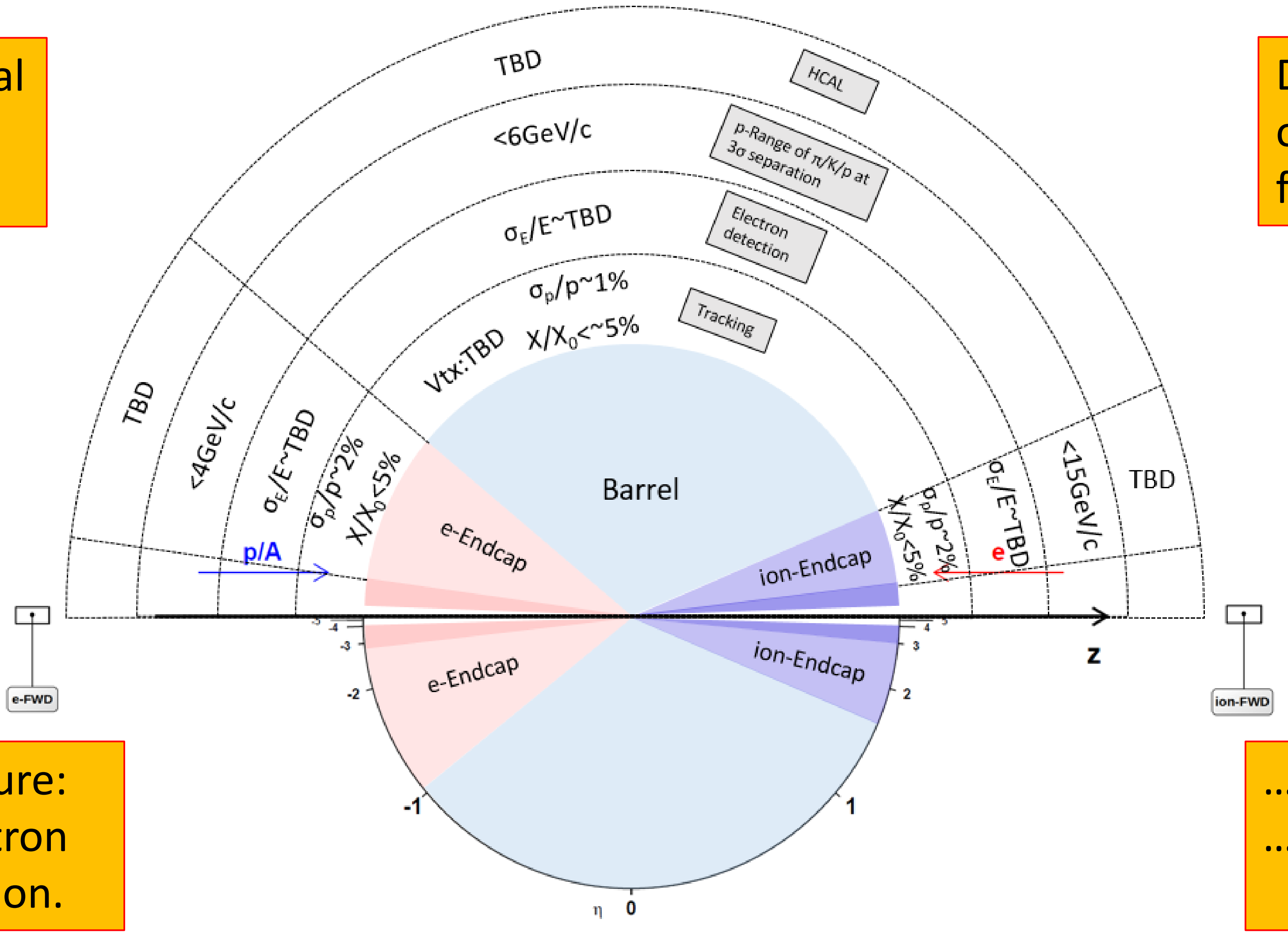

Pion/Kaon structure: detection of neutron at forward direction.

…

…

3D Structure of Nucleons

➢ Probe TMD using SIDIS

Leading Twist TMDs		Quark Polarization		
		Unpolarized (U)	Longitudinally Polarized (L)	Transversely Polarized (T)
Nucleon Polarization	U	$f_1(x,k_T^2)$ *Unpolarized*		$h_1^\perp(x,k_T^2)$ *Boer-Mulders*
	L		$g_1(x,k_T^2)$ *Helicity*	$h_{1L}^\perp(x,k_T^2)$ *Long-Transversity*
	T	$f_{1T}^\perp(x,k_T^2)$ *Sivers*	$g_{1T}(x,k_T^2)$ *Trans-Helicity*	$h_1(x,k_T^2)$ *Transversity* $h_{1T}^\perp(x,k_T^2)$ *Pretzelosity*

TMDs via SIDIS		Quark Polarization		
		Unpolarized (U)	Longitudinally Polarized (L)	Transversely Polarized (T)
Nucleon Polarization	U	$F_{UU} \propto f_1 \otimes D_1$ *Unpolarized*		$F_{UU}^{\cos(2\phi_h)} \propto h_1^\perp \otimes H_1^\perp$ *Boer-Mulders*
	L		$A_{LL} \propto g_1 \otimes D_1$ *Helicity*	$A_{UL}^{\sin(2\phi_h)} \propto h_{1L}^\perp \otimes H_1^\perp$ *Long-Transversity*
	T	$A_{UT}^{\sin(\phi_h-\phi_S)} \propto f_{1T}^\perp \otimes D_1$ *Sivers*	$A_{LT}^{\cos(\phi_h-\phi_S)} \propto g_{1T} \otimes D_1$ *Trans-Helicity*	$A_{UT}^{\sin(\phi_h+\phi_S)} \propto h_1 \otimes H_1^\perp$ *Transversity* $A_{UT}^{\sin(3\phi_h-\phi_S)} \propto h_{1T}^\perp \otimes H_1^\perp$ *Pretzelosity*

➢ **Fragmentation Functions (FF):**

D_1→Unpolarized FF, $H_1^\perp$→ Collins FF

✓ Describe the process of the struck quark fragmenting into a hadron

✓ Can be obtained from ($e + e^- \longrightarrow h^\pm + X$) data (e.g., BELLE)

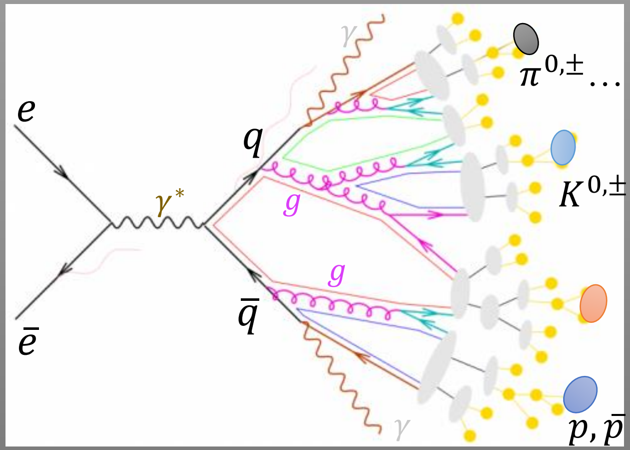

Present status of TMDs extraction

Sivers

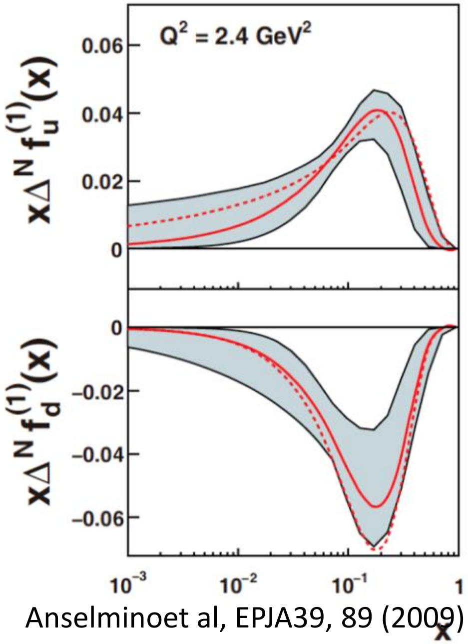

Anselminoet al, EPJA39, 89 (2009)

Transversity

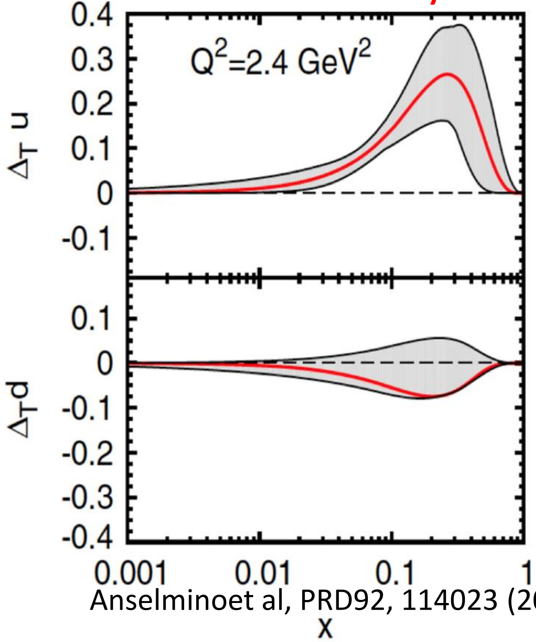

Anselminoet al, PRD92, 114023 (2015)

Pretzelosity

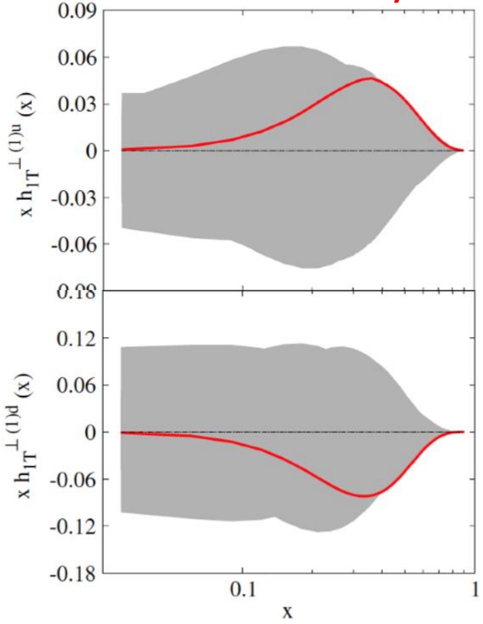

Lefkyet al, PRD91, 034010 (2015)

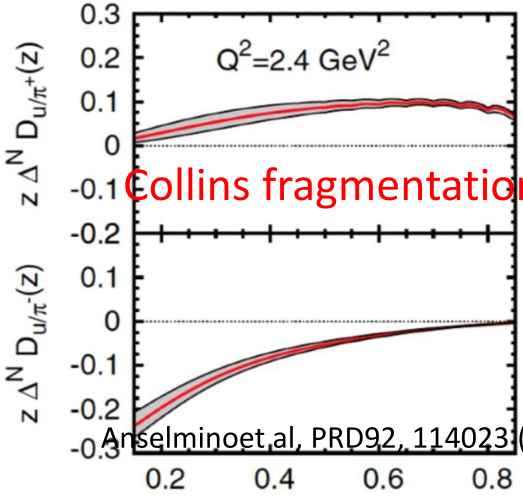

Collins fragmentation function

Anselminoet al, PRD92, 114023 (2015)

Transverse Momentum Dependent Parton Distributions

$$
\begin{aligned}
\frac{d\sigma}{dx\,dy\,dz\,dP_{hT}^2\,d\varphi_h\,d\psi} = {} & \left[\frac{\alpha}{xyQ^2}\,\frac{y^2}{2(1-\varepsilon)}\left(1+\frac{\gamma^2}{2x}\right)\right]\times\left(F_{UU,T}+\varepsilon F_{UU,L}\right)\times \\
\Bigg\{ & 1+\cos\varphi_h\times\sqrt{2\varepsilon(1+\varepsilon)}\,A_{UU}^{\cos\varphi_h}+\cos(2\varphi_h)\times\varepsilon A_{UU}^{\cos(2\varphi_h)}+ \\
& \lambda\sin\varphi_h\times\sqrt{2\varepsilon(1-\varepsilon)}\,A_{LU}^{\sin\varphi_h}+ \\
& S_L\left[\sqrt{2\varepsilon(1+\varepsilon)}\,\sin\phi_h A_{UL}^{\sin\phi_h}+\varepsilon\sin(2\phi_h)\,A_{UL}^{\sin(2\phi_h)}\right]+ \\
& S_L\lambda\left[\sqrt{1-\varepsilon^2}\,A_{LL}+\sqrt{2\varepsilon(1-\varepsilon)}\,\cos\phi_h A_{LL}^{\cos\phi_h}\right]+ \\
& \mathrm{S_T}\left[\begin{aligned}
& \sin\varphi_S\times\left(\sqrt{2\varepsilon(1+\varepsilon)}\,A_{UT}^{\sin\varphi_S}\right)+ \\
& \sin(\varphi_h-\varphi_S)\times\left(A_{UT}^{\sin(\varphi_h-\varphi_S)}\right)+ \\
& \sin(\varphi_h+\varphi_S)\times\left(\varepsilon A_{UT}^{\sin(\varphi_h+\varphi_S)}\right)+ \\
& \sin(2\varphi_h-\varphi_S)\times\left(\sqrt{2\varepsilon(1+\varepsilon)}\,A_{UT}^{\sin(2\varphi_h-\varphi_S)}\right)+ \\
& \sin(3\varphi_h-\varphi_S)\times\left(\varepsilon A_{UT}^{\sin(3\varphi_h-\varphi_S)}\right)
\end{aligned}\right]+ \\
& \mathrm{S_T}\lambda\left[\begin{aligned}
& \cos\varphi_S\times\left(\sqrt{2\varepsilon(1-\varepsilon)}\,A_{LT}^{\cos\varphi_S}\right)+ \\
& \cos(\varphi_h-\varphi_S)\times\left(\sqrt{(1-\varepsilon^2)}\,A_{LT}^{\cos(\varphi_h-\varphi_S)}\right)+ \\
& \cos(2\varphi_h-\varphi_S)\times\left(\sqrt{2\varepsilon(1-\varepsilon)}\,A_{LT}^{\cos(2\varphi_h-\varphi_S)}\right)
\end{aligned}\right]\Bigg\}
\end{aligned}
$$

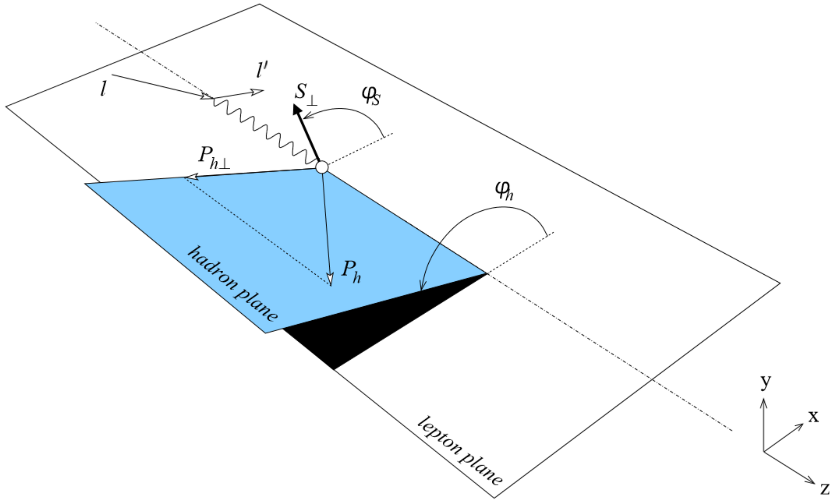

Extract TMDs from asymmetries

A.Kotzinian, **Nucl. Phys. B441**, 234 (1995). ***Bacchetta, Diehl, Goeke, Metz, Mulders and Schlegel*** *JHEP 0702:093 (2007)*

With recent progresses in [5, 6] it is possible to calculate the TMD parton distributions with Lattice QCD.

Transverse Momentum Dependent Parton Distributions

Experimental observables

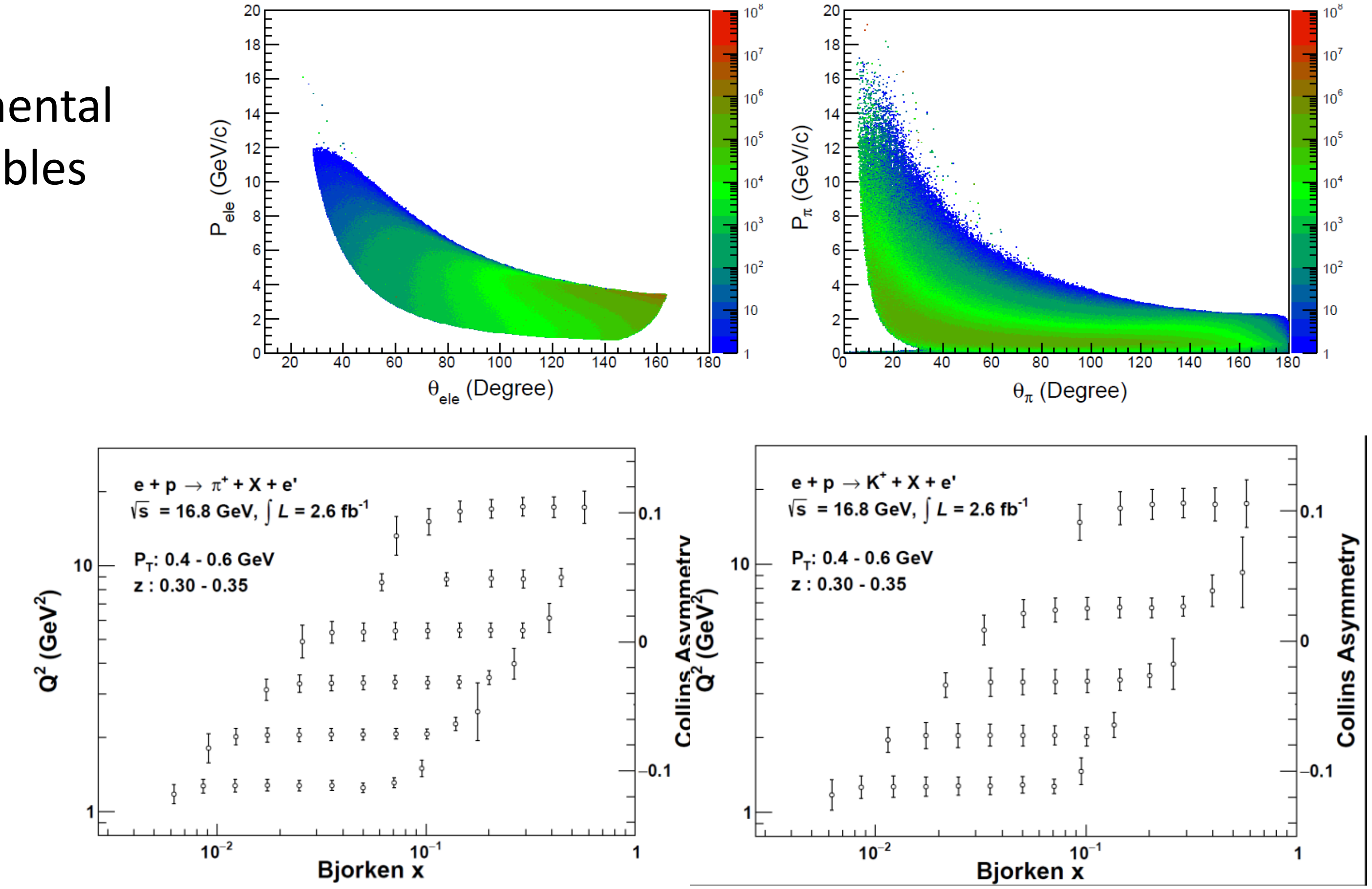

Generalized Parton Distributions (GPDs)

Eight GPDs for quarks or gluons

		Quark Polarization		
		Unpolarized (U)	Longitudinally Polarized (L)	Transversely Polarized (T)
Nucleon Polarization	U	H		$2\tilde{H}_T + E_T$
	L		$\tilde{H}$	$\tilde{E}_T$
	T	E	$\tilde{E}$	$H_T, \tilde{H}_T$

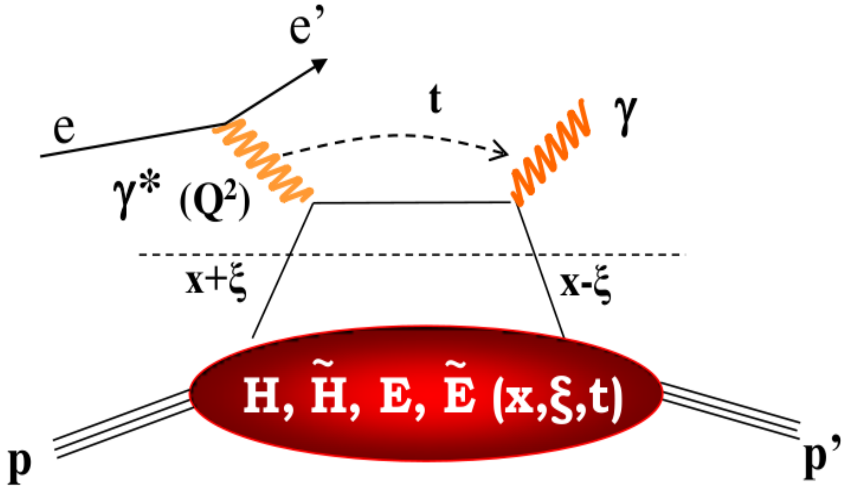

- x → Longitudinal quark momentum fraction (not experimental accessible)
- ξ → Longitudinal momentum transfer. In Bjorken limit: $\xi = x_B/(2-x_B)$
- t → Total squared momentum transfer to the nucleon: $t = (P-P')^2$

mentum

$$J^q = \frac{1}{2}\int dx\, x\left[H^q(x,\xi,t=0) + E^q(x,\xi,t=0)\right]$$

X.-D. Ji, Phys. Rev. Lett. 78 (1997) 610.

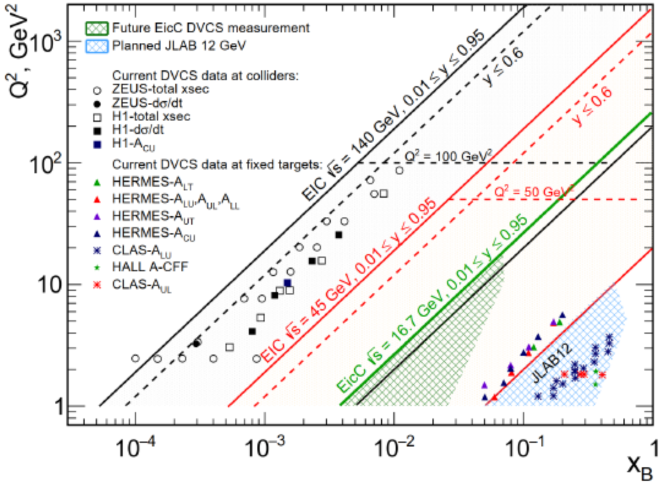

The plot shows the kinematic coverage of DVCS measurement on US-EIC and that on EicC. EicC would be a perfect machine to coverage the sea quark domain.

The projection of relative statistic uncertainties at different bins of high Q^2 on EicC, with the integrated luminosity $= 50\ \mathrm{fb}^{-1}$. HERMES data are shown with the relative statistical errors divided by a factor of 10.

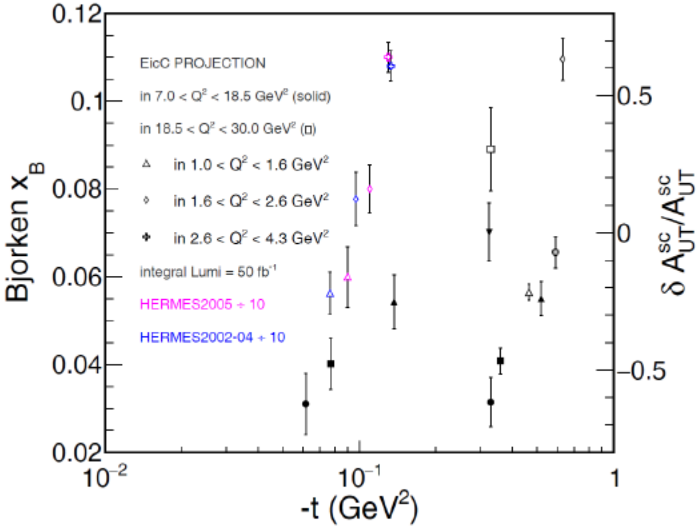

The invariant kinematical variable distribution of DVCS+BH on EicC. The binning strategy is shown in the figures below.

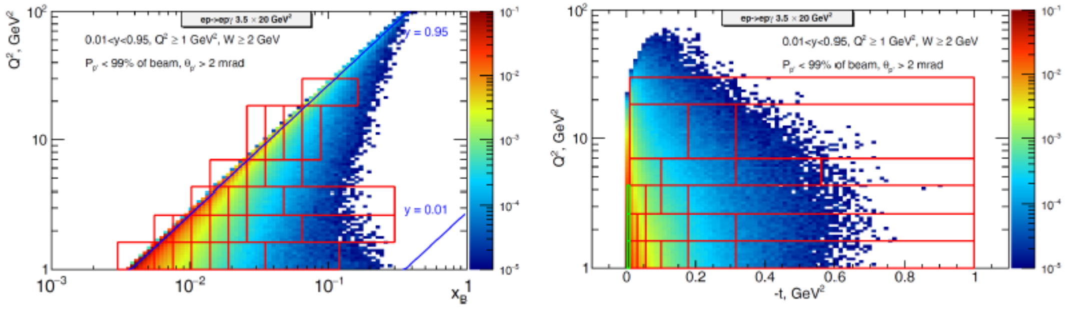

The projection of relative statistic uncertainties at different bins on EicC, with the integrated luminosity $= 50\ \mathrm{fb}^{-1}$.

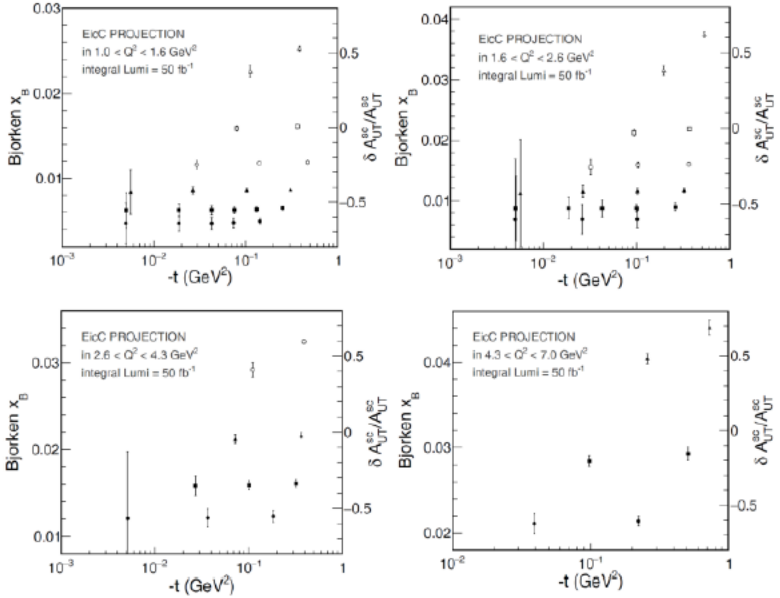

HIAF Timetable

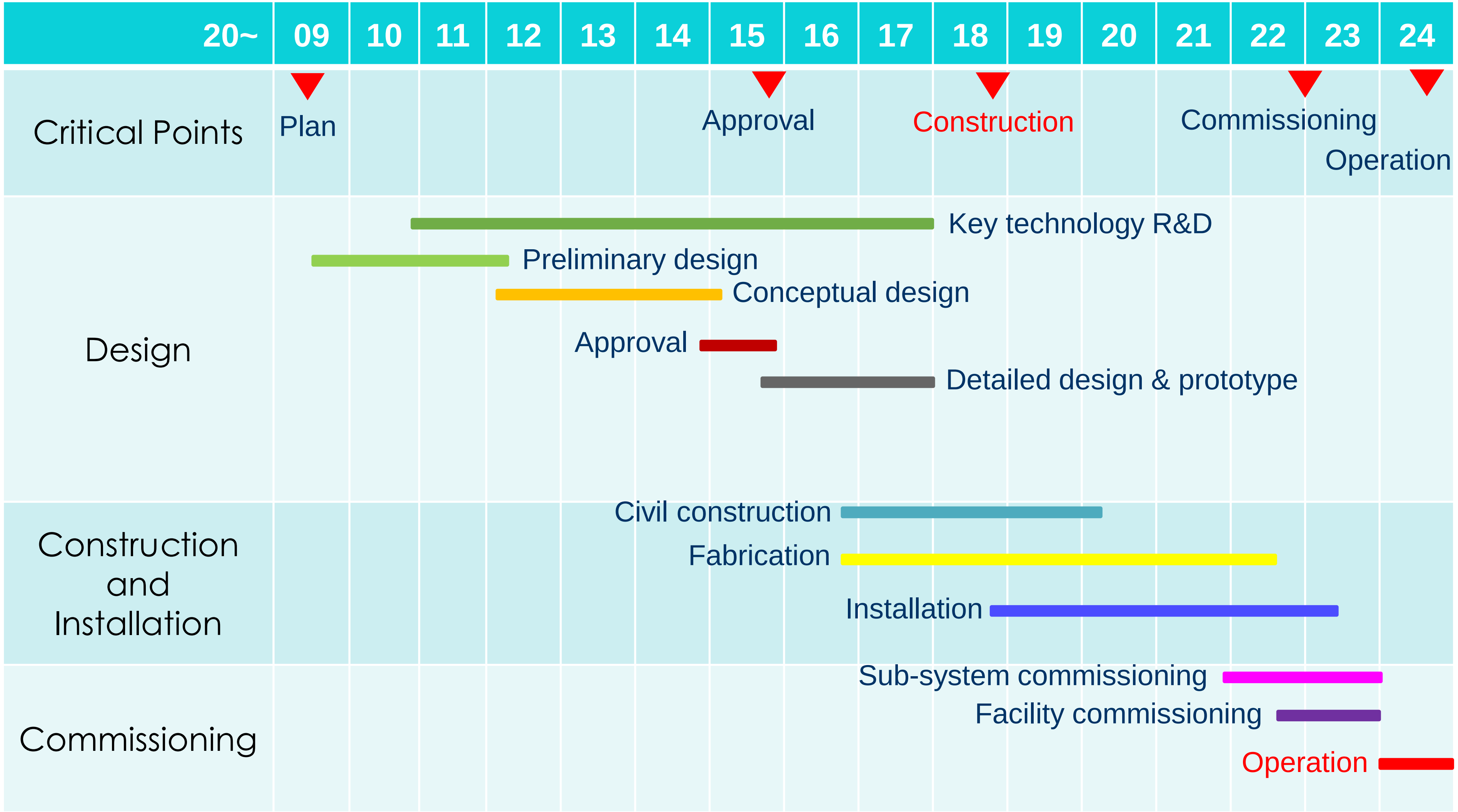

EicC 总体规划

EicC 总体方案布局

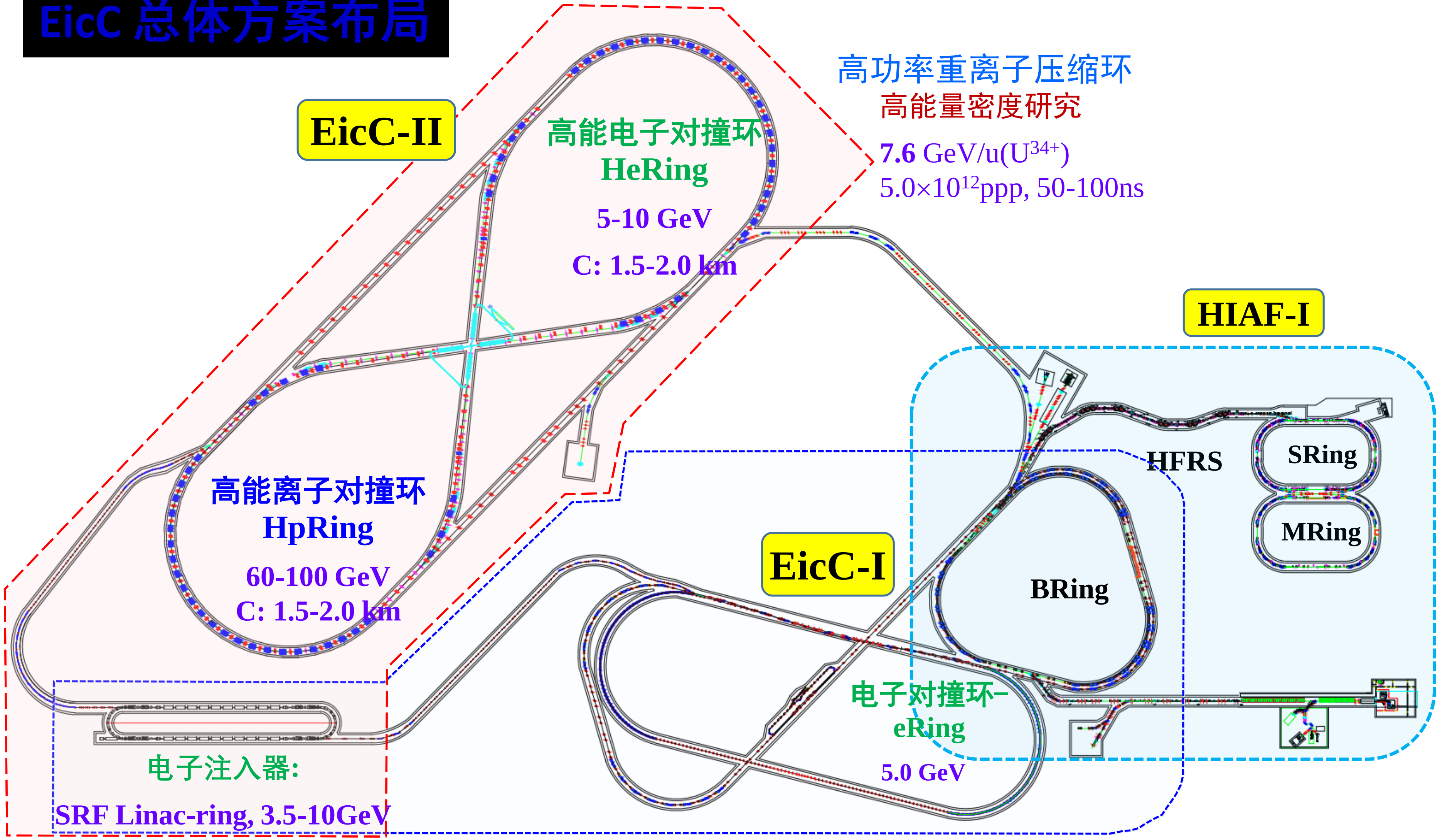

离子对撞环 - pRing

20 GeV，C: 1347 m Polarized proton

德国-HERA: 国际首台 EIC 装置

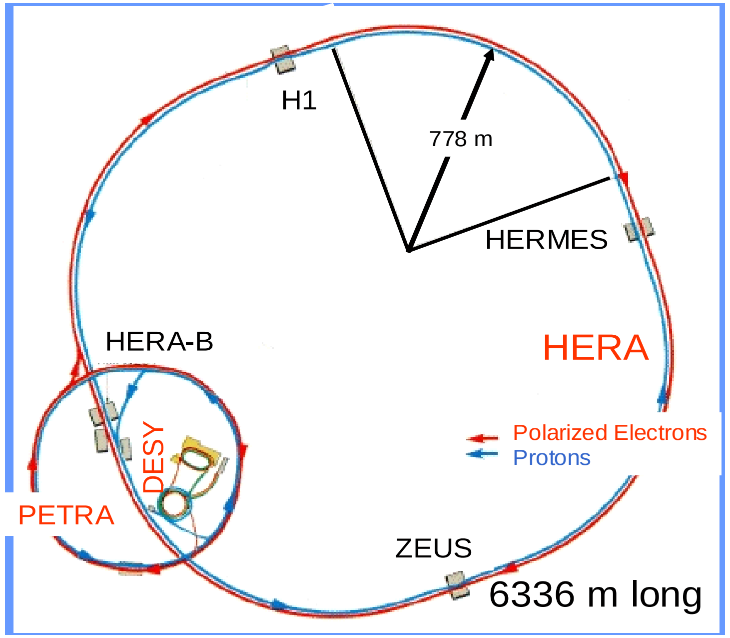

		Lepton	Proton
Energy	GeV	27.5	920
Intensities	mA	60	180×10^{11}
Magnetic field	T	0.15	1.5
Acc. voltage	MV	130	2
e-polarization	%	50 to 70	--

Final luminosity
$(1.5 \text{ to } 5) \times 10^{31}$ cm^{-2}s^{-1}

A Ring-Ring (polarized) Lepton-Proton collider with 320 GeV CM energy

1981 Proposal
1984 Start construction
1991 Commissioning, first Collisions
1992 Start Operations for H1 and ZEUS,
➔ 1st exciting results with low luminosity
1994 Install East Spin Rotators
➔ Longitudinal polarized leptons for HERMES
1996 Install 4th Interaction region for HERA-B
1999 High Luminosity Run with electrons
2000 High efficient luminosity production:100 /pb/y
2001 Install luminosity upgrade,
Spin Rotators for H1 and ZEUS
2003 Longitudinal polarization in high energy collisions
2007 End of a highly successful program

Tunnel: 5.2 m diameter

美国-BNL: eRHIC

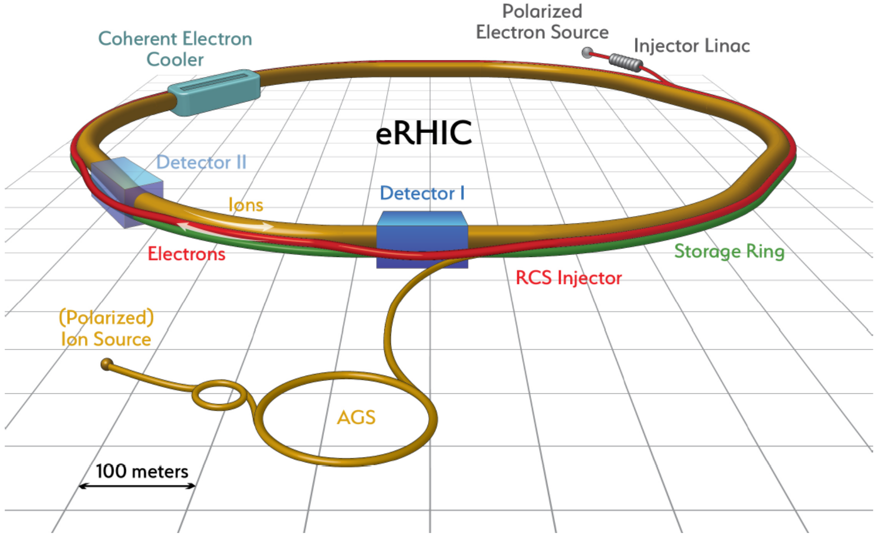

	Nominal Design (with cooling)		Risk Mitigation (no cooling)	
Species	p	e	p	E
Bunch frequency [MHz]	112.6		56.3	
Bunch intensity [10^11]	0.6	1.5	1.05	3.0
Number of bunches	1320		660	
Beam current [A]	1	2.5	0.87	2.5
Rms norm. emit. h/v [um]	2.7/0.38	391/20	4.1/2.5	391/95
Rms emittance h/v [nm]	9.2/1.3	20/1	13.9/8.5	20/4.9
β* h/v [cm]	90/4	42/5	90/5.9	63/10.4
IP rms beam size h/v [um]	91/7.2		112/22.5	
IR rms angular spread h/v [urad]	101/179	219/143	124/380	179/216
b-b parameter (/IP) h/v	0.013/0.007	0.064/0.099	0.015/0.005	0.1/0.083
Rms bunch length [cm]	5	1.9	7	1.9
Rms energy spread, 10^-4	4.6	5.5	6.6	5.5
Max space charge parameter	0.004	neglig.	0.001	neglig.
IBS growth time tr/long, h	2.1/2.0		9.2/10.1	
Polarization, %	80	70	80	70
Hourglass and crab crossing factor	0.87		0.85	
Peak luminosity [10^33 cm-2s-1]	**10.1**		**4.4**	
Integrated luminosity/week, fb^{-1}	**4.51**		**1.12**	

电子环方案：ERL，NS-FFAG

质心能量: 255GeV/p + 15.9GeV/e

$\sqrt{S}$=126GeV

设计亮度：4.4×10^{33} cm^{-2}s^{-1} –无冷却

1.0×10^{34} cm^{-2}s^{-1}-冷却

工程计划：2022-2025之间开建

美国-JLab: JLEIC

CEBAF

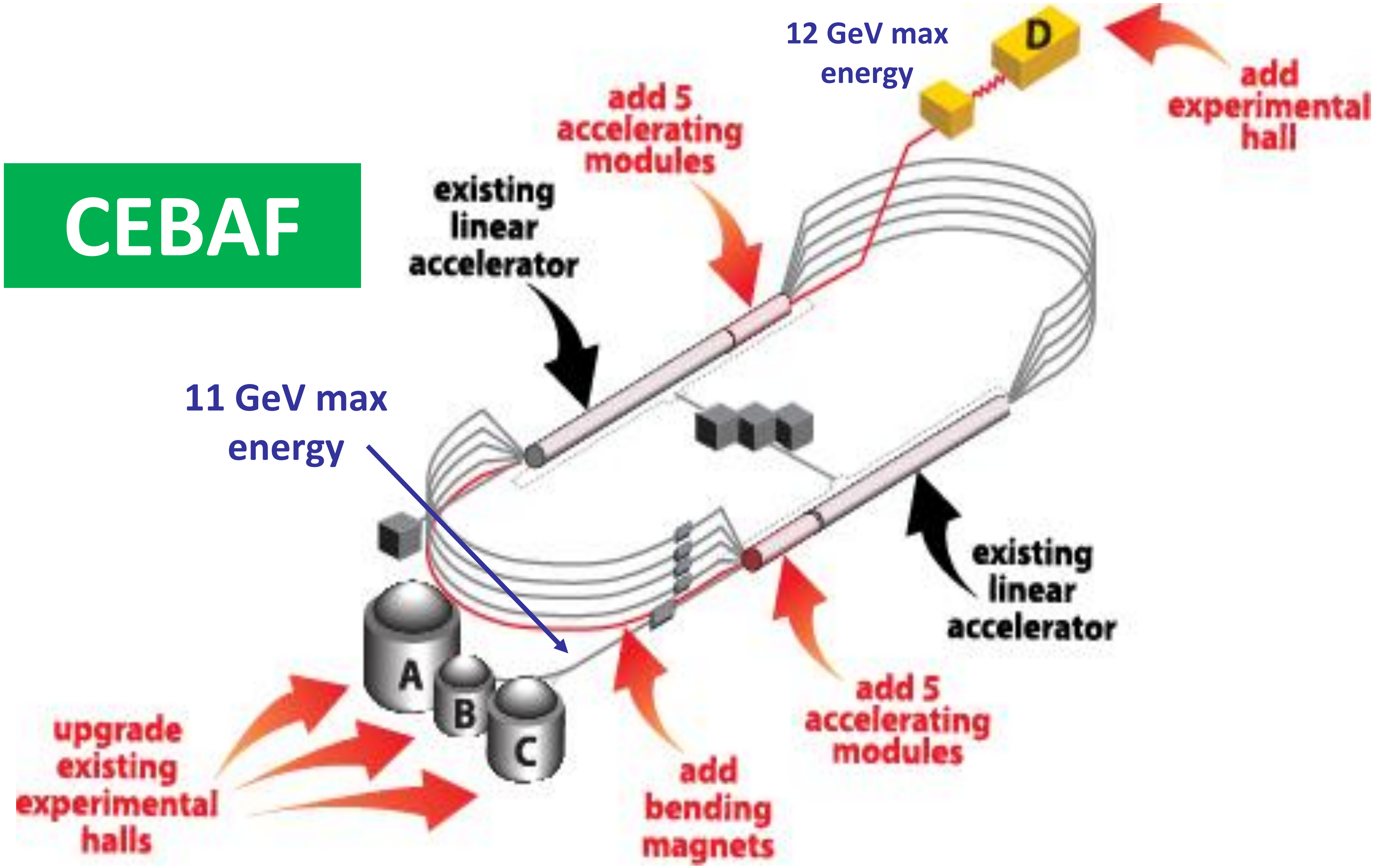

美国-JLab: JLEIC

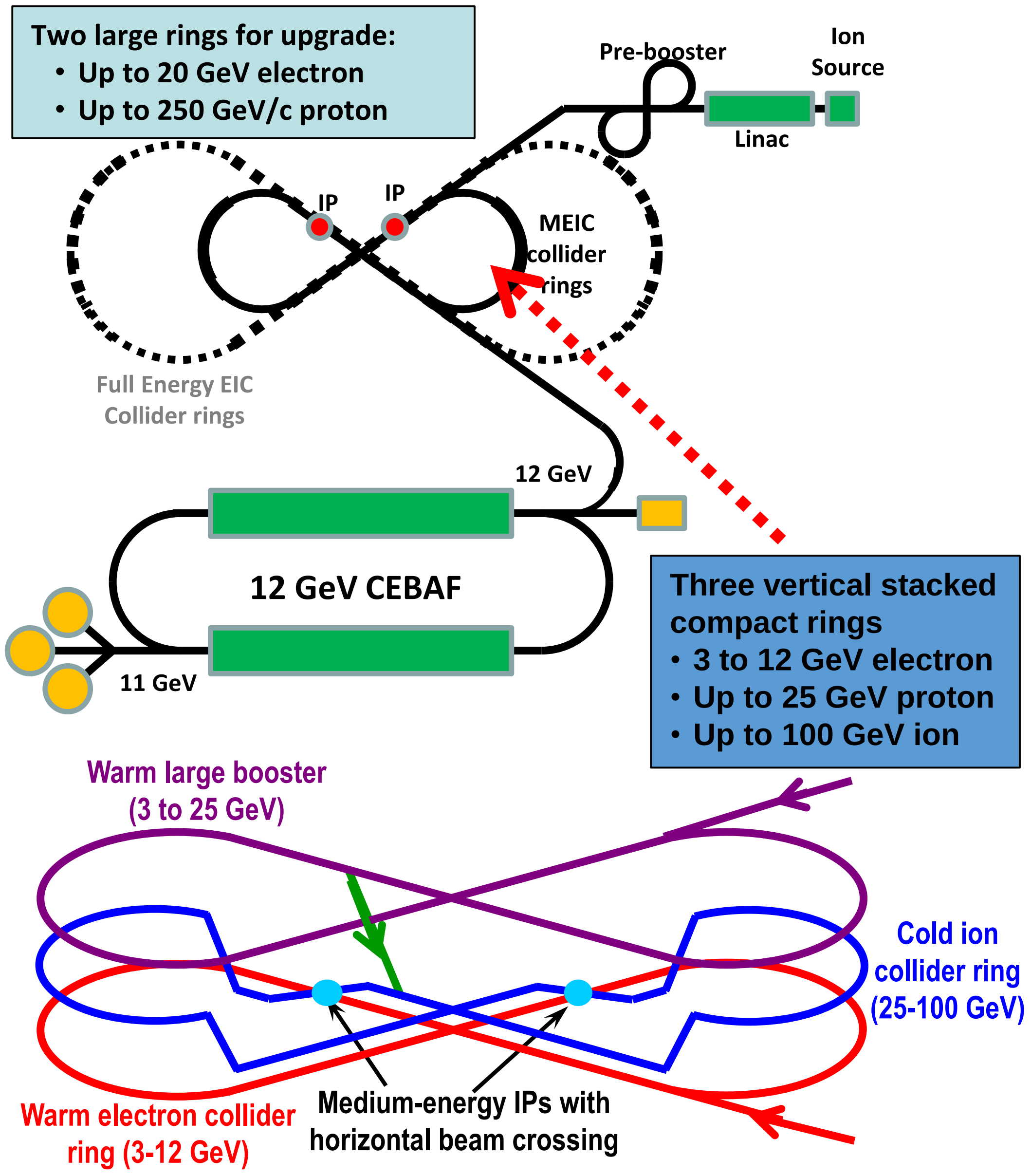

Present baseline: Ring-Ring

- Energy: 3-12 GeV e on 20-100 GeV p
  or up 40 GeV/u ion
- Polarized light ions (p, d, ^{3}He), unpolarized ions up to A=200 (Au, Pb)
- New ion complex & two collider rings
- Up to 3 interaction points
- High polarization for both beams
- Conventional electron cooling
- Upgradable to 20 GeV electron, 250 GeV proton or 100 GeV/u ion

电子环方案：“8”字型环

质心能量：60-100GeV p +
3-12 GeV e

设计亮度：5.6×10^{33} cm^{-2}s^{-1}
1.4×10^{34} cm^{-2}s^{-1}

工程计划：2022-2025方案设计

CERN: LHeC

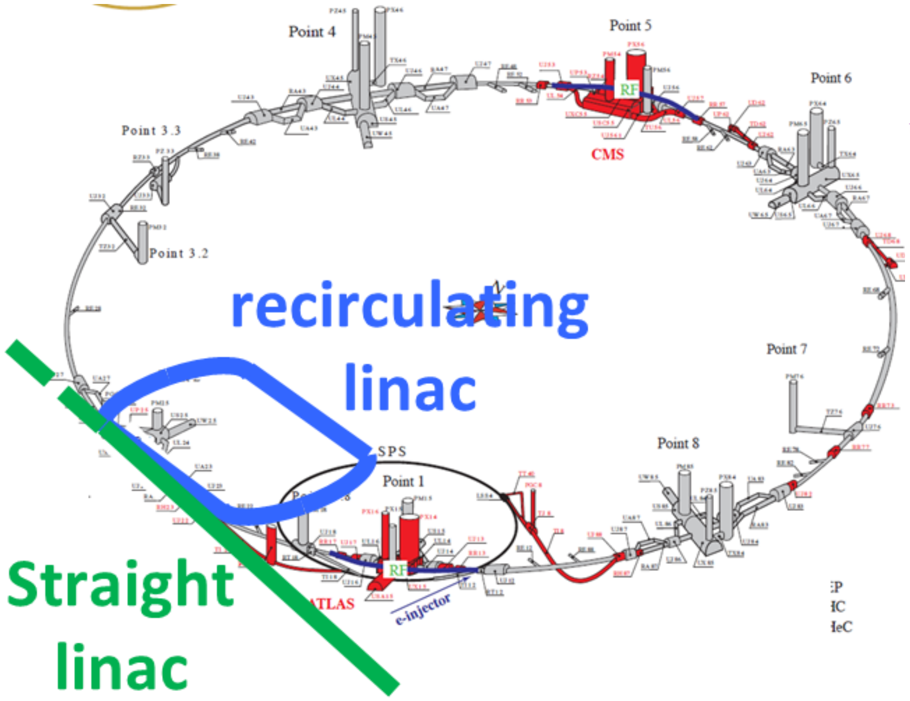

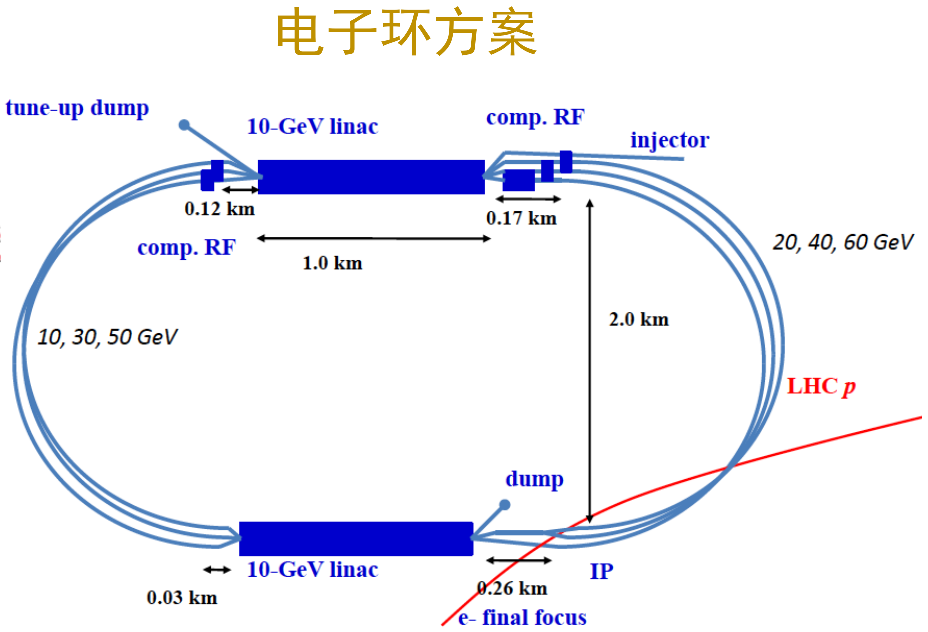

10^{34} cm^{-2} s^{-1} Luminosity reach		PROTONS	ELECTRONS
Beam Energy	GeV	7000	60
Luminosity	10^{33}cm^{-2}s^{-1}	16	16
Normalized emittance $ge_{x,y}$	mm	2.5	20
Beta Funtion $b^{*}_{x,y}$	m	0.05	0.10
rms Beam size $s^{*}_{x,y}$	mm	4	4
Beam Current	mA	1112	25
Bunch Spacing	Ns	25	25
Bunch Population	10^9	$2.2*10^{11}$	$4*10^9$
Bunch charge	nC	35	0.64

电子环方案：ERL circulator Ring

质心能量: 7 TeV p + 60 GeV e

设计亮度: 1.6×10^{34} cm^{-2}s^{-1}

工程计划：2025-2035 方案设计

国际EIC研究目标

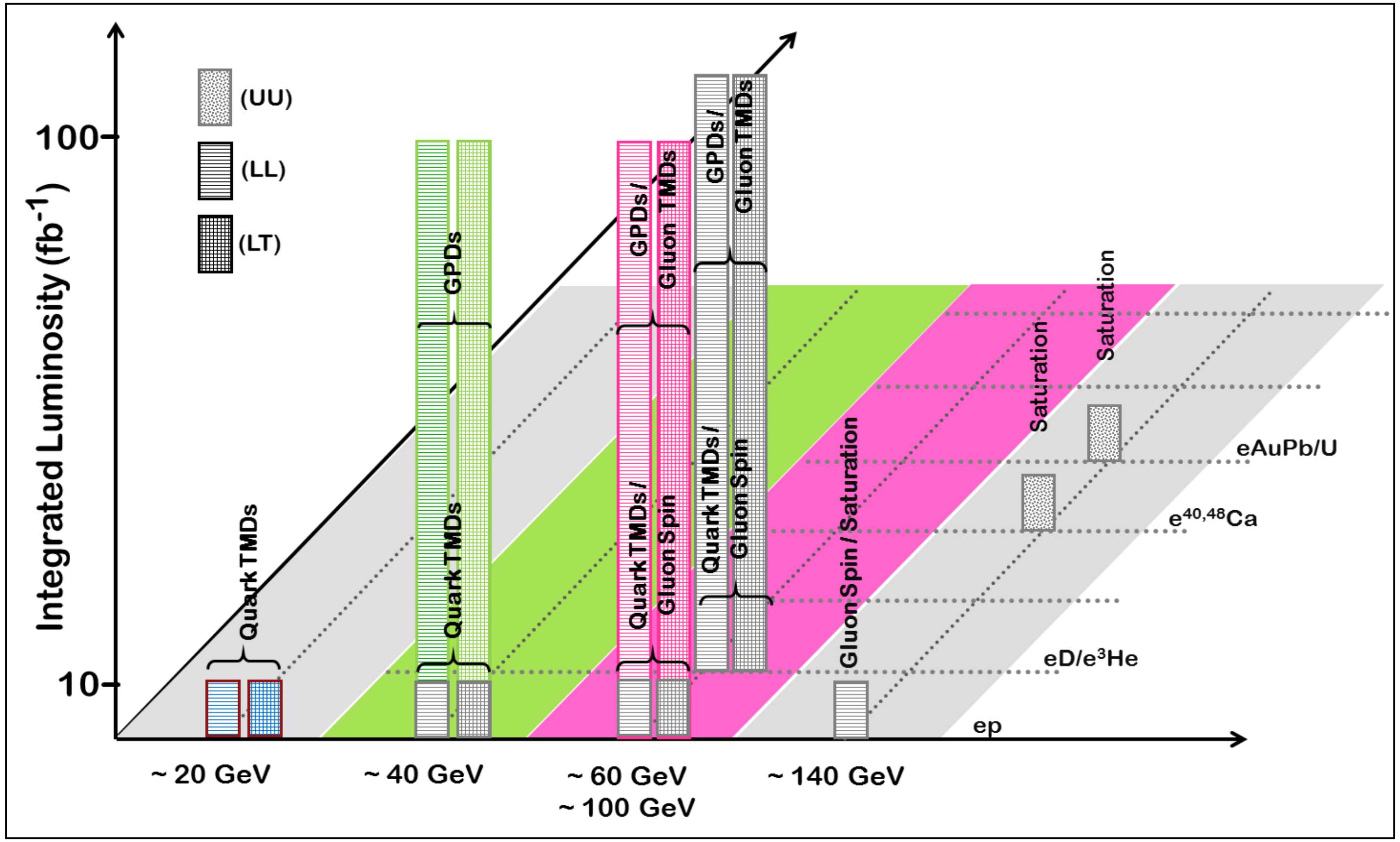

EicC	JLEIC	eRHIC	LHeC
20(p)+5 (e) GeV 100(p)+10 (e) GeV 质心能: 20/45 GeV	100(p)+5 (e)GeV 100(p)+10 (e)GeV 质心能: 45/63 GeV	255(p)+15.9(e)GeV 质心能: 126 GeV	7TeV+60GeV 非极化 质心能: 1296 GeV

The Longitudinal Spin of the Nucleon

$$\frac{1}{2} = S_q + L_q + S_g + L_g$$

$$\Delta f(x, Q^2) \equiv f^+(x, Q^2) \; - \; f^-(x, Q^2) \qquad f \, = \, u, d, s, \bar{u}, \bar{d}, \bar{s}, g$$

$$S_q(Q^2) = \frac{1}{2}\int_0^1 \Delta\Sigma(x, Q^2)dx \, \equiv \, \frac{1}{2}\int_0^1 \left(\Delta u + \Delta\bar{u} + \Delta d + \Delta\bar{d} + \Delta s + \Delta\bar{s}\right)(x, Q^2)dx$$

$$\frac{1}{2}\left[\frac{d^2\sigma^{\rightleftarrows}}{dx\,dQ^2} - \frac{d^2\sigma^{\rightrightarrows}}{dx\,dQ^2}\right] \simeq \frac{4\pi\,\alpha^2}{Q^4}y\,(2-y)\,g_1(x, Q^2)$$

$$g_1(x, Q^2) = \frac{1}{2}\sum e_q^2\left[\Delta q(x, Q^2) + \Delta\bar{q}(x, Q^2)\right]$$

EicC:

e p: 3.5 GeV 20 GeV 50fb-1

e 80% pol. p 70% pol.

e He-3: 3.5GeV 40/3 GeV/u

50fb-1 e 80% pol. He-3 70% pol.

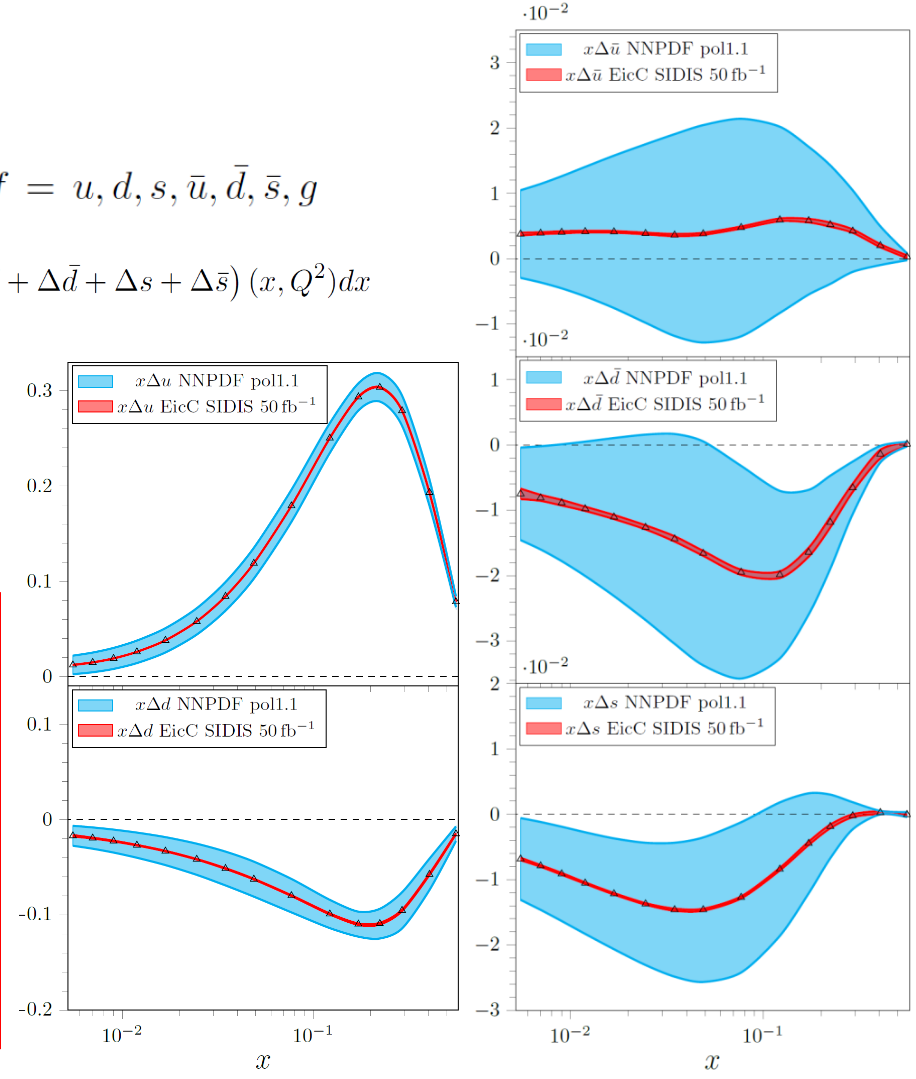

Lattice: P. Hagler, Phys. Rept. 490, 49 (2010), arXiv:0912.5483.

$$T^{\mu\nu} = \frac{1}{2}\bar{\psi} i \overleftrightarrow{D}^{(\mu}\gamma^{\nu)}\psi + \frac{1}{4}g^{\mu\nu}F^2 - F^{\mu\alpha}F^{\nu}{}_{\alpha},$$

First of all, let me decompose the $T^{\mu\nu}$ into traceless and trace parts,

$$T^{\mu\nu} = \bar{T}^{\mu\nu} + \hat{T}^{\mu\nu}, \tag{7}$$

where $\bar{T}^{\mu\nu}$ is traceless. According to Eq. (4), I have,

$$\langle P|\bar{T}^{\mu\nu}|P\rangle = (P^{\mu}P^{\mu} - \frac{1}{4}M^2 g^{\mu\nu})/M, \tag{8}$$

$$\langle P|\hat{T}^{\mu\nu}|P\rangle = \frac{1}{4}g^{\mu\nu}M. \tag{9}$$

Combining Eq. (6) with the above three equations, I get,

$$\langle \bar{T}^{00}\rangle = \frac{3}{4}M, \tag{10}$$

$$\langle \hat{T}^{00}\rangle = \frac{1}{4}M. \tag{11}$$

Thus 3/4 of the nucleon mass comes from the traceless part of the energy-momentum tensor and 1/4 from the trace part. The magic number 4 is just the space-time dimension. This

The traceless part of the energy-momentum tensor can be decomposed into the contribution from the quark and gluon parts,

$$\bar{T}^{\mu\nu} = \bar{T}_q^{\mu\nu} + \bar{T}_g^{\mu\nu}, \tag{12}$$

$$\langle \bar{T}_q^{00} \rangle = \frac{3}{4} a(\mu^2) M,$$
$$\langle \bar{T}_g^{00} \rangle = \frac{3}{4} (1 - a(\mu^2)) M.$$

Finally, I turn to the trace part of the energy-momentum tensor $\hat{T}^{\mu\nu}$. According to Eq. (5), I decompose it into $\hat{T}_m^{\mu\nu}$ and $\hat{T}_a^{\mu\nu}$, the mass term and trace anomaly term, respectively. Both operators are finite and scale independent. If I define,

$$b = 4\langle \hat{T}_m^{00} \rangle / M, \tag{20}$$

then according to Eq. (11), the anomaly part contributes,

$$\langle \hat{T}_a^{00} \rangle = \frac{1}{4}(1 - b) M. \tag{21}$$

Thus, the energy-momentum tensor $T^{\mu\nu}$ can be separated into four gauge-invariant parts, $\bar{T}_q^{\mu\nu}$, $\bar{T}_g^{\mu\nu}$, $\hat{T}_m^{\mu\nu}$, and $\hat{T}_a^{\mu\nu}$. They contribute, respectively, $3a/4$, $3(1-a)/4$, $b/4$, and $(1-b)/4$ fractions of the nucleon mass. The corresponding breakdown for the hamiltonian is, $H_{\rm QCD} = H'_q + H_g + H'_m + H_a$, with

$$H'_q = \int d^3\vec{x}\ \left[\bar{\psi}(-i\mathbf{D}\cdot\alpha)\psi + \frac{3}{4}\bar{\psi}m\psi\right],$$

$$H_g = \int d^3\vec{x}\ \frac{1}{2}(\mathbf{E}^2 + \mathbf{B}^2),$$

$$H'_m = \int d^3\vec{x}\ \frac{1}{4}\bar{\psi}m\psi,$$

$$H_a = \int d^3\vec{x}\ \frac{9\alpha_s}{16\pi}(\mathbf{E}^2 - \mathbf{B}^2).$$

$$H_q = \int d^3\vec{x}\ \bar{\psi}(-i\mathbf{D}\cdot\alpha)\psi,$$

$$H_m = \int d^3\vec{x}\ \bar{\psi}m\psi,$$

then the QCD hamiltonian becomes,

$$H_{\text{QCD}} = H_q + H_m + H_g + H_a.$$

Here H_q (Eq. (26)) represents the quark and antiquark kinetic and potential energies and contributes $3(a-b)/4$ fraction of the nucleon mass. H_m (Eq. (27)) is the quark mass term and contributes b fraction of the mass. H_g (Eq. (23)) is the normal part of the gluon energy and contributes $3(1-a)/4$ fraction of the mass. Finally, H_a (Eq. (25)) is the gluon energy from the trace anomaly. It contributes $(1-b)/4$ fraction of the mass.

TMD

$$
\begin{aligned}
&\frac{d\sigma}{dx\,dy\,d\psi\,dz\,d\phi_h\,dP_{h\perp}^2} \\
&\quad = \frac{\alpha^2}{xyQ^2}\,\frac{y^2}{2\,(1-\varepsilon)}\left(1+\frac{\gamma^2}{2}\right) \\
&\quad \times \Bigg\{ F_{UU,T} + \varepsilon F_{UU,L} + \sqrt{2\,\varepsilon(1+\varepsilon)}\,\cos\phi_h\,F_{UU}^{\cos\phi_h} + \varepsilon\cos(2\phi_h)\,F_{UU}^{\cos 2\phi_h} \\
&\qquad + \lambda_e\,\sqrt{2\,\varepsilon(1-\varepsilon)}\,\sin\phi_h\,F_{LU}^{\sin\phi_h} + S_\parallel\left[\sqrt{2\,\varepsilon(1+\varepsilon)}\,\sin\phi_h\,F_{UL}^{\sin\phi_h} + \varepsilon\sin(2\phi_h)\,F_{UL}^{\sin 2\phi_h}\right] \\
&\qquad + S_\parallel\lambda_e\left[\sqrt{1-\varepsilon^2}\,F_{LL} + \sqrt{2\,\varepsilon(1-\varepsilon)}\,\cos\phi_h\,F_{LL}^{\cos\phi_h}\right] \\
&\qquad + |\boldsymbol{S}_\perp|\Bigg[\sin(\phi_h-\phi_S)\left(F_{UT,T}^{\sin(\phi_h-\phi_S)} + \varepsilon\,F_{UT,L}^{\sin(\phi_h-\phi_S)}\right) + \varepsilon\,\sin(\phi_h+\phi_S)\,F_{UT}^{\sin(\phi_h+\phi_S)} \\
&\qquad\quad + \varepsilon\,\sin(3\phi_h-\phi_S)\,F_{UT}^{\sin(3\phi_h-\phi_S)} + \sqrt{2\,\varepsilon(1+\varepsilon)}\,\sin\phi_S\,F_{UT}^{\sin\phi_S} \\
&\qquad\quad + \sqrt{2\,\varepsilon(1+\varepsilon)}\,\sin(2\phi_h-\phi_S)\,F_{UT}^{\sin(2\phi_h-\phi_S)}\Bigg] \\
&\qquad + |\boldsymbol{S}_\perp|\lambda_e\Bigg[\sqrt{1-\varepsilon^2}\,\cos(\phi_h-\phi_S)\,F_{LT}^{\cos(\phi_h-\phi_S)} + \sqrt{2\,\varepsilon(1-\varepsilon)}\,\cos\phi_S\,F_{LT}^{\cos\phi_S} \\
&\qquad\quad + \sqrt{2\,\varepsilon(1-\varepsilon)}\,\cos(2\phi_h-\phi_S)\,F_{LT}^{\cos(2\phi_h-\phi_S)}\Bigg]\Bigg\},
\end{aligned}
$$

One particular example is the quark Sivers function $f_{1T}^{\perp q}$ which describes the transverse momentum distribution correlated with the transverse polarization vector of the nucleon. As a result, the quark distribution will be azimuthally asymmetric in the transverse momentum space in a transversely polarized nucleon. Figure 2.13 demonstrates the deformations of the up and down quark distributions. There is strong evidence of the

Sivers effect in the DIS experiments observed by the HERMES, COMPASS, and JLab Hall A collaborations [71, 72, 73]. An important aspect of the Sivers functions that has been revealed theoretically in last few years is the process dependence and the color gauge invariance [74, 75, 76, 77]. Together with the Boer-Mulders function, they are denoted as naive time-reversal odd (T-odd) functions. In SIDIS, where a leading hadron is detected in coincidence with the scattered lepton, the quark Sivers function arises due to the exchange of (infinitely many) gluons between the active struck quark and the remnants of the target, which is referred to as final state interaction effects in DIS. On the other hand, for the Drell-Yan lepton pair production process, it is due to the initial state interaction effects. As a consequence, the quark Sivers and Boer-Mulders functions differ by a sign in these two processes. This non-universality is a fundamental prediction from the gauge invariance of QCD [75]. The experimental check of this sign change is currently one of the outstanding topics in hadronic physics, and Sivers functions from the Drell-Yan process can be measured at RHIC.

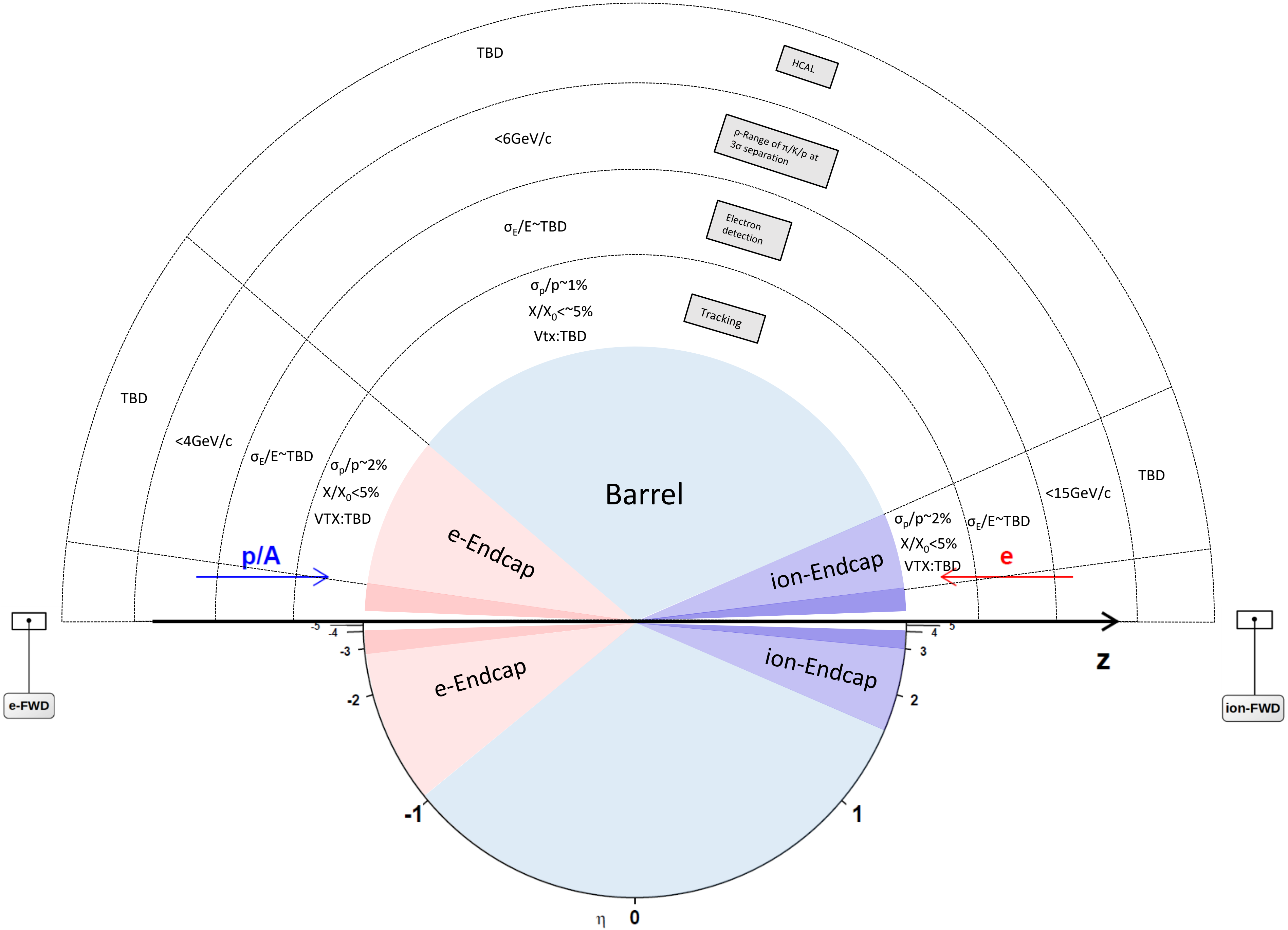

TBD
HCAL
<6GeV/c
p-Range of π/K/p at 3σ separation
σ_E/E~TBD
Electron detection
σ_p/p~1%
X/X_0<~5%
Vtx:TBD
Tracking
TBD
<4GeV/c
σ_E/E~TBD
σ_p/p~2%
X/X_0<5%
VTX:TBD
p/A
Barrel
e-Endcap
ion-Endcap
σ_p/p~2%
X/X_0<5%
VTX:TBD
σ_E/E~TBD
<15GeV/c
TBD
e
z
e-FWD
ion-FWD
e-Endcap
ion-Endcap
η
0
1
-1
2
-2
3
-3
4
-4
5
-5

The Longitudinal Spin of the Nucleon

$$\frac{1}{2} = S_q + L_q + S_g + L_g$$

$$\Delta f(x, Q^2) \equiv f^+(x, Q^2) - f^-(x, Q^2) \qquad f = u, d, s, \bar{u}, \bar{d}, \bar{s}, g$$

$$S_q(Q^2) = \frac{1}{2}\int_0^1 \Delta\Sigma(x, Q^2)dx \equiv \frac{1}{2}\int_0^1 \left(\Delta u + \Delta\bar{u} + \Delta d + \Delta\bar{d} + \Delta s + \Delta\bar{s}\right)(x, Q^2)dx$$

$$\frac{1}{2}\left[\frac{\mathrm{d}^2\sigma^{\rightleftarrows}}{\mathrm{d}x\,\mathrm{d}Q^2} - \frac{\mathrm{d}^2\sigma^{\rightrightarrows}}{\mathrm{d}x\,\mathrm{d}Q^2}\right] \simeq \frac{4\pi\,\alpha^2}{Q^4} y\,(2-y)\,g_1(x, Q^2)$$

$$g_1(x, Q^2) = \frac{1}{2}\sum e_q^2\left[\Delta q(x, Q^2) + \Delta\bar{q}(x, Q^2)\right]$$

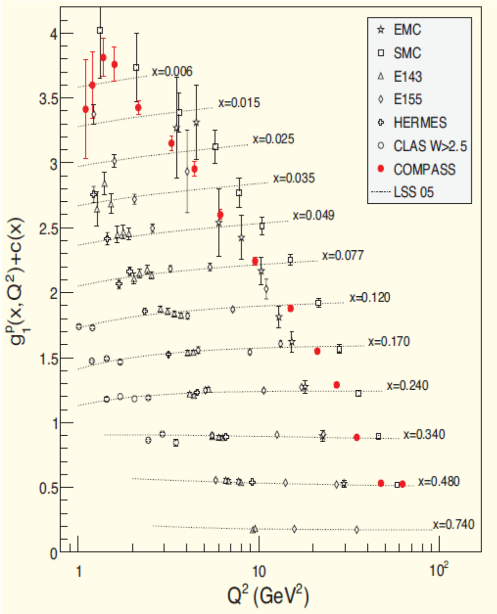

Lattice: P. Hagler, Phys. Rept. 490, 49 (2010), arXiv:0912.5483.

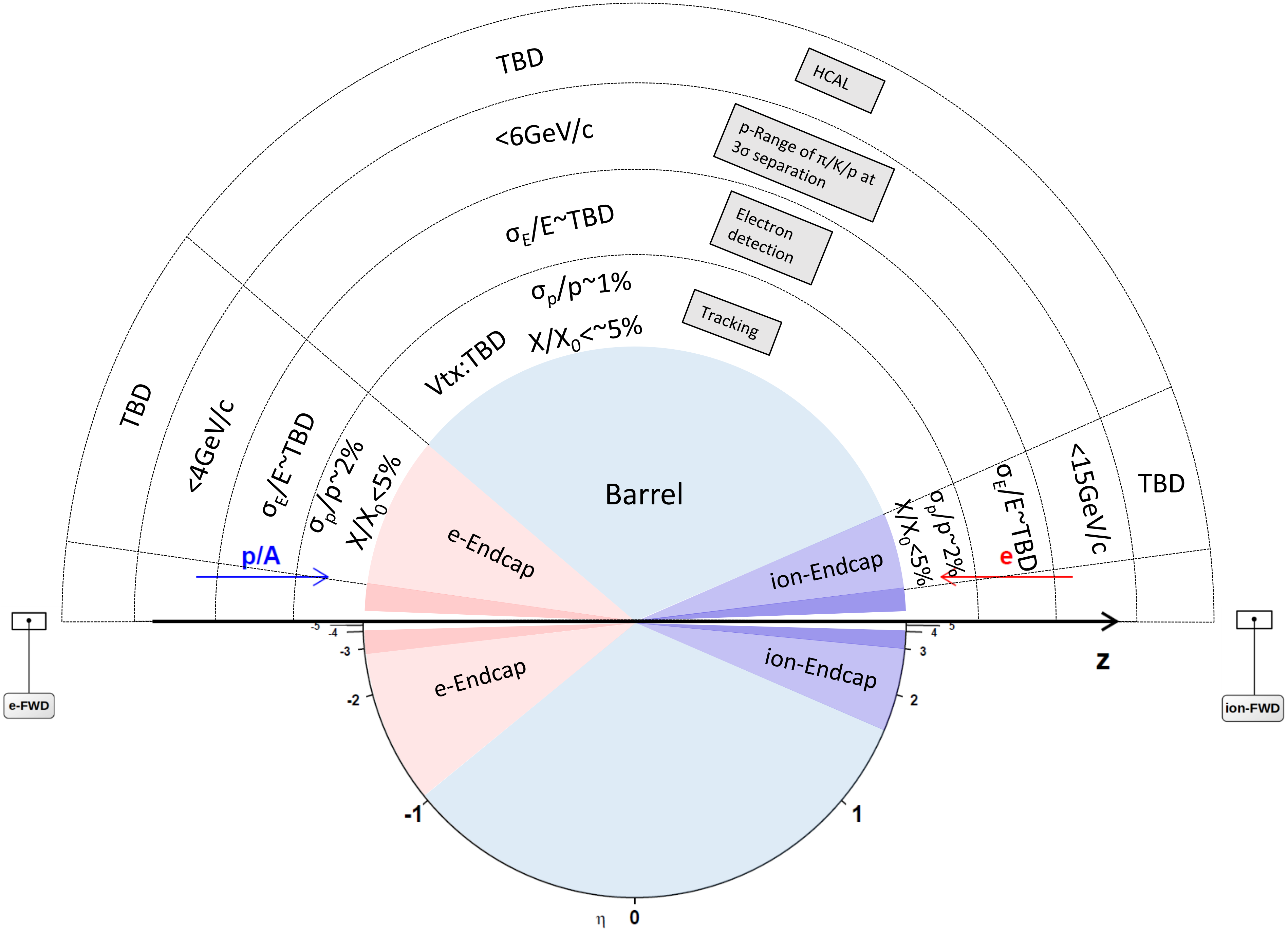

TBD
HCAL
<6GeV/c
p-Range of π/K/p at 3σ separation
σE/E~TBD
Electron detection
σp/p~1%
Tracking
X/X0<~5%
Vtx:TBD
TBD
<4GeV/c
σE/E~TBD
σp/p~2%
X/X0<5%
p/A
e-Endcap
Barrel
ion-Endcap
X/X0<5%
σp/p~2%
σE/E~TBD
<15GeV/c
TBD
e
z
e-Endcap
ion-Endcap
e-FWD
ion-FWD
-5
-4
-3
-2
-1
η
0
1
2
3
4
5